INTEGRATED GEOPHYSICAL METHODS IN BASE METAL EXPLORATION AND STUDIES OF SHEAR STRUCTURES IN KATTA II, WOLLEGA

A Thesis

Presented to

School of Graduate Studies

Addis Ababa University

In Partial Fulfillment,

of the Requirements for the Degree of

Master of Science in Applied Geophysics

by

Alemayehu Berhe

June, 1998

LIST OF FIGURES

ACKNOWLEDGMENT

My first expression of gratitude is due to the members of the Katta research project, especially Dr. Tilahum Mammo, Dr. Tigistu Haile, and Dr. Getnet Mewa for their help in arranging the field work and covering my entire field expense. I should also like to thank them for theirs a helpful and detailed list of amendments and advice throughout the preparation of the thesis.

In the Ethiopian Geological survey (EGS) I benefited greatly from the generosity of the librarians and the staff's of the library information service. I am grateful to the EGS for permission to reproduce parts of the maps used here and pe: mission to use the IP/Resistivity date on Katta..

It is a pleasure also to acknowledge the help of friends and relatives, especially Ato Kassay Kebede at Africa sun Enterprise, Ato Mulat Tegegn, and W/t Haimanot Yirga. Further, I owe a particular debt to W/ro Emebet Abraham for her patient preparation of the type script.

ABSTRACT

The Katta II area is situated in the western wollega, about 7 km east of the Nejo two. This area belongs to the Nejo series metasedimentry metavolcanic and intrusive rocks of the Upper Proterozoic metamorphosed in the greenschist facies. Phyllite, different types of schists including graphitic schist, quartzite, gossaniferrous and metavolcanic are the prevalent rock types in Katta II.

A large number of geological investigation and borehole drilling in Katta II were carried out in the years between 1970 and 1982. As a result, occurrences of copper, zinc, lead, gold and cobalt are reported.

The purpose of this paper is mainly to outline the concepts of using integrated geophysical data to delineate the position of structural features and identify the base metal mineralization zone and thereby determining the most probable locations of economic importance. For this purposes reevaluation of the existing IP/resistivity data and detailed magnetic and EM surveys were done. The results of the qualitative interpretation are presented and discussed in relation to the available geological, geochemical and borehole information. The interpretation is made on the bases of experimental, theoretical, and field model curves. Preliminary results show that shear structures control the mineralization. The investigation further indicates that the abundance of graphitic schist in the study area causes serious interpretational problem.

For thorough understanding of the anomalous zones and their qualitative description, frequency domain IP, gravity, radiometric surveys and quantitative interpretation of the magnetic data are proposed.

1. INTRODUCTION

1.1 Previous works, purpose of investigation and method of approach

Reports indicate that an Italian Group was prospecting for gold in the vicinity of Nejo before world war II (Wahi, 1982). Even so, interest in Katta area has actually begun to grow in late 60's and early 70's after UN mineral surveyors found out geochemical anomalies of Cu, Zn and Ni minerals. Since then, the area has met a mixed fortune to be closely watched by several geologists and geochemists. Fairly large numbers of works, more than 20 in number, have been carried out in the years between 1970 and 1982; almost all of which were geological and geochemical in nature. For the better understanding of the level of mineralization, few boreholes were sunk on Katta-II area and the log interpretations for the core samples are presented (Belay, 1978; Tilahun, 1980; Ball, 1982). Though limited in number, geophysical reports are also available. The UNDP Mineral Exploration Programs in Ethiopia conducted extensively a two stage geophysical reconnaissance survey between 1976 and 1980 (Wahi, 1982).

In the first stage, IP/Resistivity surveys were carried out during the field season 1976–1977 using dipole-dipole electrode configuration at 100 m electrode spacing. Magnetic survey at 20m picket interval was also undertaken during the same field season to study the nature of the conducting zones and the regional geological and structural pattern.

The second stage of the reconnaissance survey continued in the 1979–1980 field season. During this period, More detailed Self-Potential surveys along 6 profiles and IP/Resistivity surveys, using a 3-pole (pole-dipole) configuration, along profiles 200S, 300S and 400S (Fig. 4) executed to cover both the previously delineated IP and geochemical anomaly zone in Katta II. In this survey, successful use of integrated geophysical methods brought out significant exploration outcomes.

In general, the works done at all levels have been extensive and the time and financial resource devoted were estimated to be quite large. The research result so far accomplished is, however, by no means conclusive enough. A number of geological maps are available for the area, but none of them seem complete and disparities in a number of geological facts exist among themselves. Beyond qualitative assessment of individual nature, no research work has yet been tried to outline the level of mineralization and structural setup of the area by compiling and correlating all available data in one set.

The complex geology of the area coupled with uncoordinated work of engaging in similar undertakings mainly accounts for the incomplete knowledge about the area. The problem has become even worsen, when the trend of tectonics zones are delineated solely from geological and geochemical considerations without having enough exposures in such structurally complicated area. Nevertheless, relatively better geological and geochemical information is available while very little is known about geophysical signatures of the area.

As a step towards making up for this gap, this study is concerned with:

-the application of integrated geophysical methods to examine and map the subsurface structure of the Katta II locality and

-to investigate the association of the base metal with these geological settings.

To accomplish the stated objectives, a two phase extensive investigation has been performed. In the first phase, a preliminary desk study concentrate on reviewing and re-evaluation of the available geological, geochemical and geophysical information up to reprocessing, reinterpretation and correlation of the results with the geological and borehole data of already existing IP/Resistivity and magnetic data. This initial phase also includes designing of detailed EM and magnetic survey along selected profiles that require further investigation in the Katta II. The area was chosen not only on considering the re-revaluation result but also on the fact that it is reasonably well documented through 6-diamond drill holes and their core log interpretation.

Field survey, processing and interpretation of the newly acquired data, and integrated interpretation of the entire results was undertaken in the second phase of the research work. Evaluation regarding the usefulness of the methodologies in detecting and delimiting the ore bodies and the structural zones with effectiveness, level of correlation and correspondence, etc., is outlined based on results of this study.

2. GEOLOGY

2.1 Location, Accessibility and Morphology

Katta II district, which covers an area of about 2.5 sq.km, is located 7 km east of Nejo town in Western Wollega (Fig-1). The area is situated in the Ethiopian highlands at elevations of about 1800 to 2000 m above sea level, and is drained by a network of narrow tributaries of the Dilla River. Steeper hills and narrow valleys cover the area. Thick overburden, composed of red and reddish brown lateritic soil, mainly occupy the section between the top of the hills and the bottom of the valleys. The town of Nejo at a distance of 515 from Addis Ababa, is accessible by an all-whether road partially with asphalt up to Nekemte. But one can reach to the survey area which is 7 km from Nejo, following older cleared tracks by four-wheel drive car during the dry season only. The area is very sparsely populated and the topography is rugged and highly dissected by a number of streamlines rendering it difficult to ground geophysical survey.

2.2 Regional Geology

The Pan-African system of mobile zones from late Proterozoic to early Paleozoic comprises of the longer region of tectono-thermal activity covering much of northeast Africa that extends from the northern end of Red sea to Ethiopia, including the neighboring Arabian Shield. The region is right along strike of the Pan–African Mozambique Belt and is a direct continuation of it (Park, 1995). The Mozambique Belt contains large areas of older continental basement yielding Archean to mid-Proterozoic

ages and is variably affected by the Pan-African deformation and metamorphism with ages ranging from C. 950 to 550 Ma. The rock assemblages in the Mozambique belt in the East African sector consist of granitoid gneisses with widespread and abundant intercalations of metasediments including quartzites, marbles, and graphitic pelites---The metasedimentary assemblage as a whole probably represents a continental shelf sequence with an original eastward facies changing from near shore sands to deep-water limestones, resting on older granitoid basement now transformed to gneiss. To the north, however, contemporaneous rocks of the Arabian–Nubian shield are largely obscured by thick volcanic sequences and related intrusivs of calcalkaline character that blanket much of the area (Camp, 1984). This together with scattered occurrences of ophiolitic lithologies initiated several workers to interpret the region on the light of tectonic models in spite of the disputing role of plate tectonic process in Precambrian time.

The Pan-African tectonothermal activity represents a period from c. 1200 Ma to c. 450 Ma BP, that is, from mid Proterozoic to lower Paleozoic, and divides into periods each marked by an orogenic event. Gass referred to them as lower, middle and upper Pan–African (Park, 1995). The older rocks of the Lower Pan-African are of the middle Proterozoic (between 1200 Ma BP and 900 Ma BP) metasedimentary quartzites overlain by thick sequences of basalts and basaltic andesites with oceanic affinities intercalated with graywacke carbonates and charts. The Middle Pan African orogeny (between 900 Ma and 660 Ma) is marked by bulk plutonic rocks of gabbroic-to-granitic composition that often form N-S to NE–SW trending broad linear zones. These zones are interpreted as the roots of volcanic island arcs. On the other hand, a series of unmetamorphosed and

undeformed silicic volcanic and volcanoclastic sediments represent the upper Pan African igneous rocks of the region.

Outcrops of older continental crust in Ethiopia have been identified in four areas (Kazmin, 1971). In his study of the stratigraphical subdivision of Precambrian deposits in southern and western Ethiopia, Kazmin recognized three main lithological complexes referred to as the lower, middle and upper. Most of the western part of Wollega region forms part of the upper complex that comprises of very thick succession of geosynclinal formations marked by comparatively light metamorphism, restricted granitization and a specific type of structure. Part of the Birbir Series of the upper complex in which Katta is situated, consists of chlorite and sericite schists with interbedded quartzites, graphitic rocks, acid and basic volcanics and siliceous rocks. Iron-bearing quartzites as well as intraformational conglomerates are also reported. These rocks are followed by a thick units of phyllites, sometimes containing fine grained kyanite and staurolite, with interbedded biotitized sandstones and quartzites.

Fig. 1

LOCATION MAP

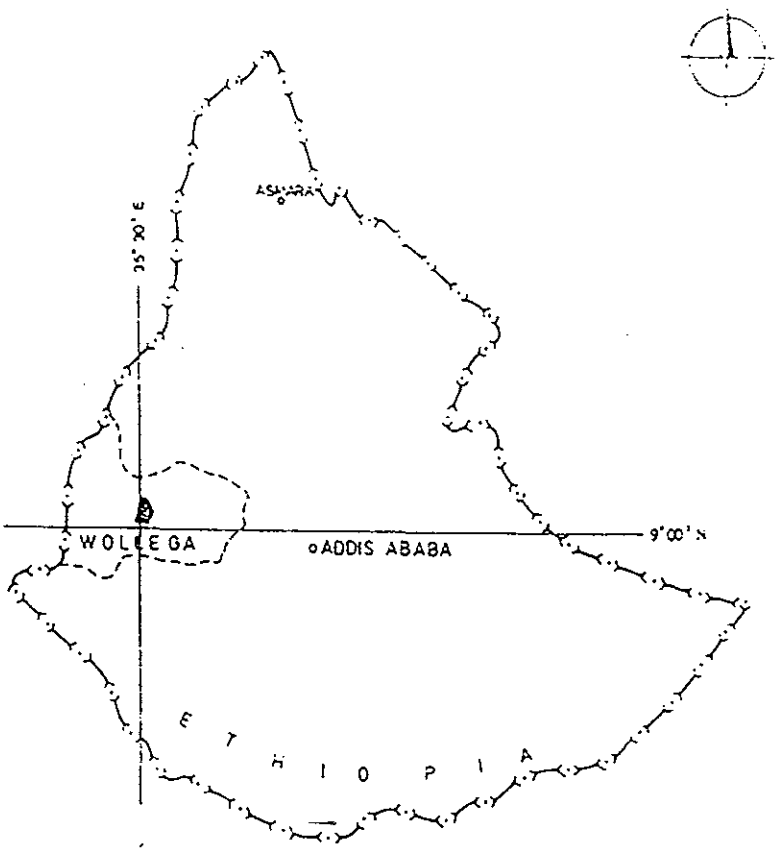

AREA UNDER STUDY

0 500 km

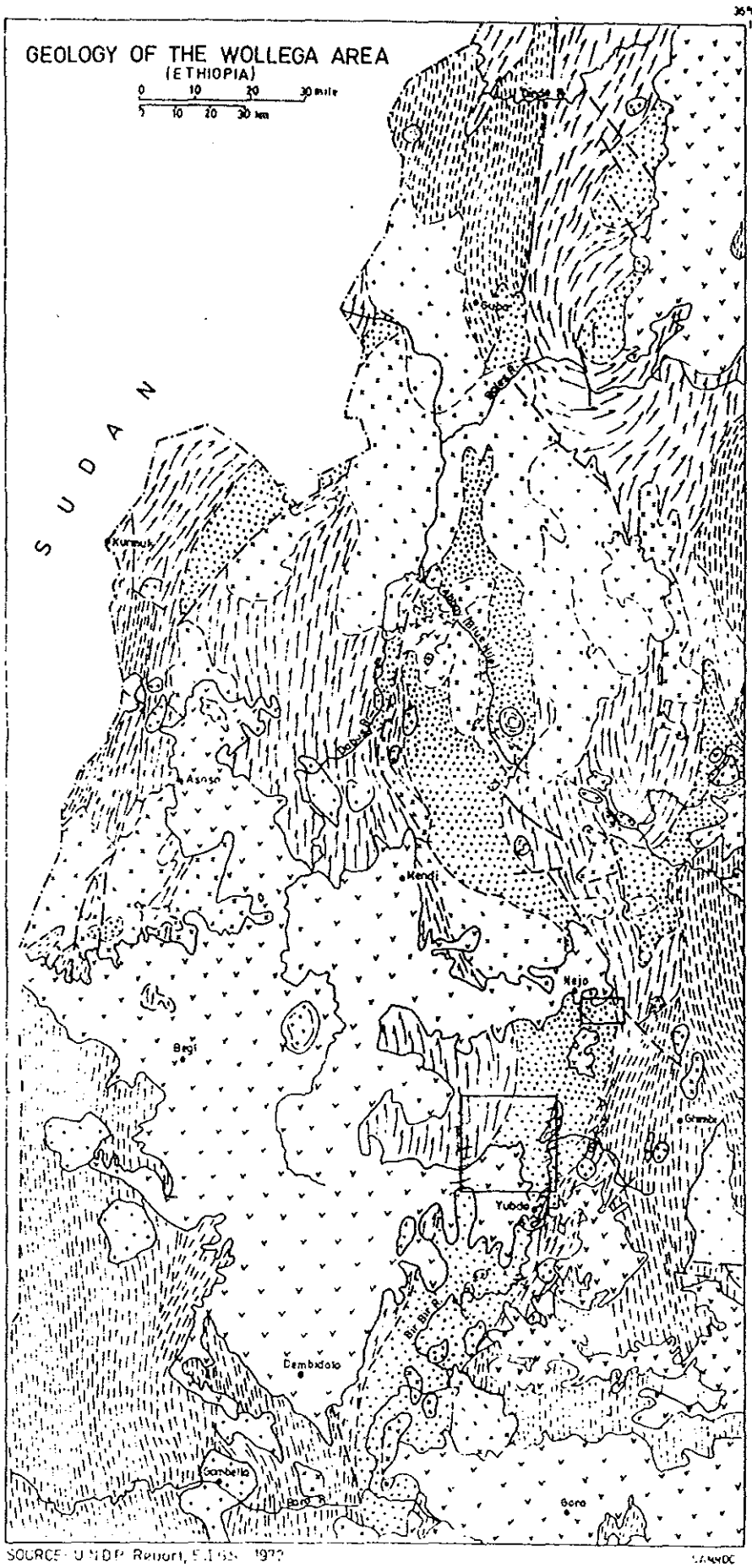
GEOLOGY OF THE WOLLEGA AREA
(ETHIOPIA)
0 10 20 30 mile
5 10 20 30 km
36°00'
12°00'
SUDAN
Kumruk
Asosa
Kendi
Nejo
Begi
Gimbi
Yubdo
Dembidolo
Gambella
Baro R.
Gore
Neogene-Quaternary volcanics
Bir-Bir group
Metavolcanic group
Gneisses-Lower complex
Post-tectonic granites and granodiorites
Syenites
Syntectonic granites and granodiorite
Gabbro
Ultrabasics
Faults
Contacts a) certain b) supposed
Ring complexes
Kato Area

Fig. 2

2.3 LOCAL GEOLOGY

Different people have tried to describe the Geology of Katta area at various times (Tilahun, 1980; Soukhoroukov, 1982, etc). However, a relatively complete description of Katta II area, particular interest of this study, is given by Soukhoroukov. The map on Fig.3 shows the simplified geological sketch of the Katta II area adapted from the geological map of Abo–Kami–Katta area compiled by Soukhoroukov. Katta II, located about 7 km east of Nejo, belongs to the Nejo Series metasedimentary metavolcanic and intrusive rocks of the Upper Proterozoic metamorphosed in the greenschist facies (Ibid). From field observations as well as from previous geological and geochemical findings phyllite, schist, quartze, metavolcanic rocks and gossan are the prevalent rock types of Katta II.

Three varieties of phyllites outcrops so far recognized in the area are conglomeratic, tuffaceous and graphitic phyllites (soukhoroukov, 1982). Quartzite ridges lying comformably with the general strike were encountered in several places within phyllites, green schists and quartz-sericite schists. Passing to the northwest edge of Katta II and south of Katta basalt hill (Fig. 3) the area is covered by outcrops of schists overlaying the intrusive body. Outcrops of metadiorite and metagranodiorite intrusives that presumably belong to one big intrusive unit are found along the streams. Gossaniferous schists also outcrop along the western margin of the greenschists, east of Katta II. Geochemical surveying along this zone brought out copper mineralization as high as 3200 PPM, and indicated a definite strike pattern over a length of about 300 meters (Wahi, 1982).

The drilling carried out at Katta II has added a great deal of information about the subsurface geology. Belay (1978), Tilahun (1980), Ball (1982) have given log interpretation on selected samples. Particularity, Tilahun, in his MSc Thesis, has given the full treatment for five bore hole core logging results, their stratigraphic correlation, petrographic studies of the rocks and orebodies, and depth variation in mineralogy. Accordingly, repetitive succession of different units of similar lithologies have been obtained from petrographic studies. In general, varieties of phyllites and schists of different composition and structure and intrusive bodies were encountered in succession comprising dominantly of schits.

The nature of mineralization in the Katta area has been classified as syngenetic and epigenetic types (Tilahun, 1980). In the syngenetic type, stratiform mineralization occurs mainly within a sericite chlorite schist unit and is formed in island arc environments in which much of the volcanism was submarine. In the epigenetic type, mineralization is formed as a result of remobilization, recrystalization and concentration of the already existing minerals. They are vein and disseminated type and supposed to be the main type of mineralization in the area.

The rocks have undergone different episodes of intense penetrative deformation resulting in folding and faulting (Tilahun, 1980; de wit, 1977). The effect of folding in phyllites, which mainly form the rocks of the Katta area, is recognized as anticlinal structure, plunging south. Folds of different amplitude, western 65°-30° dip and submeridian 10^0-34^0 strike, were observed in phyllites and greenschists (Soukhoroukov, 1982).

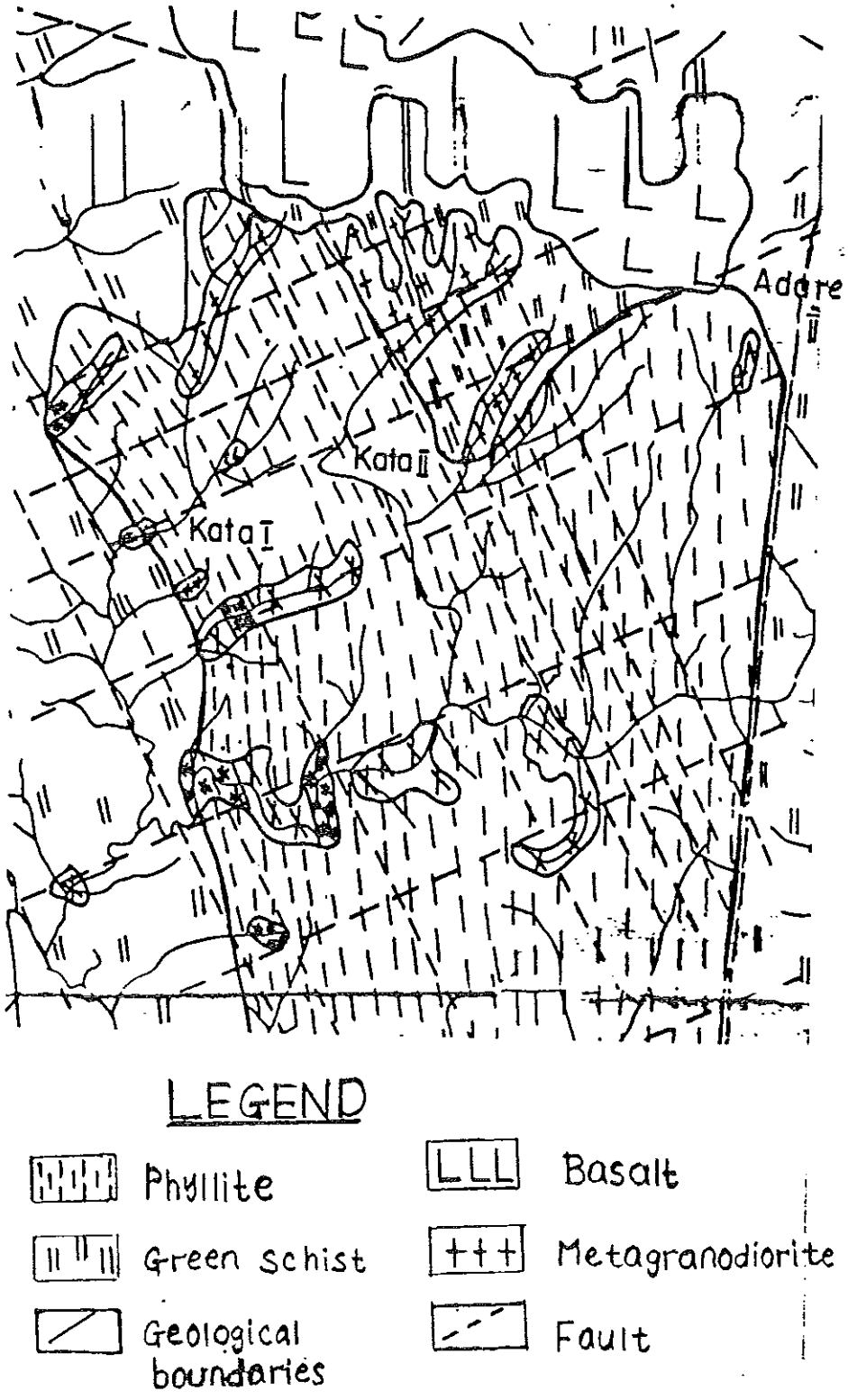

Fig. 3 Geology Map of Katta II

3. IP AND RESISTIVITY SURVEYS

3.1 An overview of the base metal mineralization and Geophysical prospecting

The art of prospecting for suitable metallic minerals from carefully selected sites to make tools and weapons have begun since stone age. Gold, copper, bronze, silver, and later iron are the earliest metals used to produce tools, weapons and ornaments during the advent of the ancient civilization in Egypt, Mesopotamia, China and elsewhere. But, consumption was significantly increased after industrial revolution. Even so, the use of base metals during most of the 19th Century was extremely low by present day standards. After the turn of the present century, industrialization spread rapidly and this created an increasing demand for the traditional base metals like copper, tin, lead and zinc. There was also an increased use of the new base metals, nickel and aluminum, as a result of an increased application, as a major structural metal, replacing steel in many of its traditional roles; in electrical industry, aircraft industry, domestic appliance manufacture and packaging.

To meet this rising demand for base metals in industry, it would be necessary to make a continual search for a new deposits and extensions to those which have so far been in use. This will in effect demand the use of more efficient and cost effective exploration techniques. Application of integrated geophysical methods, which have been in great

stride of growth and development in instrumentation, field technique, and interpretation, have proven useful and accurate in discovering the majority of the world base metal mines. Before reviewing the use of geophysical methods in prospecting for base metal deposits, it is necessary to describe and discuss the general features and types of stratified sulphide deposits as a good knowledge of these is essential in designing geophysical exploration program in search of deposits of this type.

The sulphide minerals are of primary importance in base metal exploration since they include metallic ore minerals that are principal sources of copper, zinc, lead and nickel. They occur in various geological settings as a result of different geological processes. Though there seems to exist two classes of thoughts on the origin of formative solutions, the general mechanisms for the formation of post magmatic base metals follow a natural sequence of the cooling of hydrothermal solutions which arise as a result of differentiation from magma containing rather average quantities of the base metals and water, a sufficiently high concentration of chloride and sufficient sulfur to precipitate (Holland, 1972).

Volcanic associated stratified sulphide deposits that are very profitable to exploit are typically lenticular to sheetlike in shape and broadly stratiform and are often composed of pyrite, pyrrhotite, with less amount of chalcopyrite, sphalerite and galena; and chalcocite. Arsenopyrite and magnetite may also be present in minor amount (William et al, 1995). Different authors have classified these ore bodies in different major groups on the bases of composition, age and lithological association. Some also object the division and consider them to be part of one continuous spectrum. Since the division can readily

render summary description of the deposits in useful form for exploration purpose, pursuing the classification will have practical significance.

The first group is the Cu–Zn type which is further divided into two subgroups. The primitive type, which constitutes the first subgroup, is mainly developed in the Archean green-stone belts. They often occur within the upper more felsic portion of basaltic to rhyolitic volcanic piles in a limited stratigraphic horizon. The second subgroup is associated with the early part of the main calc-alkaline stage of island arc formation. Those occur in successions of mafic volcanic in complex structural settings characterized by thick greywacke sequences. They are typified by deposits in the age range from early Proterozoic to Paleozoic. The cuperious pyrite type in copper rich, lead deficient areas are found in association with basic volcanic piles in the form of ophiolites and presumably formed at oceanic or back arc spreading. They are of Phanerozoic age. The last group, but not least, is the pb-zn-cu type. This group, often carrying gold and silver, is generally associated with bimodal suits, tholeiitic basalts, calcalkaline lavas and pyroclastics. Members of this group are formed in geologic age range from early Proterozoic to Phanerozoic (Holland, 1972; William et al, 1995).

While describing the syngenetic and epigenetic nature of sulphidle mineralization in Katta, Tilahun (1980) has mentioned that the former created the latter type as a result of late metamorphism and supergene remobilization. The morphologies of the orebody, the ore environment and geological time in which the syngenetic deposits were formed, are highly related to the Cu–Zn type of hydrothermal sulfide deposits mentioned earlier. For further information on the sulphide mineralization in Katta II, the reader is referred to a detailed discussion by Tilahun (1980). These deposit types mostly exhibit consistent mineralogical

zonation. In the first type, sediment of pyrite tuffite zone that is generally enriched in sphalerite is formed on top of pyrite–sphalerite mineralization. Passing stratigraphically downward follow a mineralized zone of banded pyrrhotite–pyrite–chalcopyrite–sphalerite orebodies underlain by concentrated chalchopyrite with pyrrhotite–pyrite+magnetite at the bases of the massive sulphide lens (Holland, 1972; William et al, 1995).

Subsurface geological information is effectively acquired from surface measurements of physical properties in several ways. By the same token, the nature of mineral deposits and structural patterns can be examined by studying the response of these materials to artificially and naturally applied fields. These diagnostic responses can be effectively utilized to delineate mineralized zones, distinguish the nature of mineralization in grade and size, outline the structure of rocks and intrusives and course of tectonic zones, etc. Geophysical methods not only accomplished these but also are more rapid and useful for successful planning, remove heavy physical labor, preserve the natural environment from damage, etc. Regardless of the stated advantages, it is impossible to study every square kilometer of a vast area by geophysical methods. This would be too expensive and time consuming. Geophysical exploration program for base metal mineralization should, therefore, be guided by prospecting criterion which directly or indirectly suggest the presence of the required deposit. Under prospecting criterion, geology, geochemistry, mining history if it ever exists, and by and large the physical property contrast between the ore body sought and the host rock should be given due considerations in order to delimit the area of interest and choose the geophysical methods appropriate for the specific exploration program at hand. In this evaluation program, all available relevant

data that have been acquired for various reasons should be reevaluated, reprocessed, interpreted.

The methods in geophysical exploration that are found highly effective when base metals are being sought are the electrical and magnetic methods. In electrical methods, the fact that the mineralized zones have low resistivity, high conductivity and high IP effect are used as a criterion in exploration. However, the use of the magnetic method for base metal exploration uses the magnetic ore environment as a marker or useful pathfinder in the search for sulphide minerals. Certain types of magnetic ores, especially magnetite, ilmenite, and pyrrhotite are found in association with sulphide deposits that produce distortions in the earth's magnetic field. While interpreting magnetic anomalies, it is necessary to note that many geological structures, faults, contact zones, igneous intrusives other than ore bodies can produce magnetic anomalies.

In the following subsequent sections, We shall review the electrical and magnetic methods of geophysical prospecting employed to study the base metal mineralization in Katta II in more detail with particular emphasis on the field data acquisition, processing and interpretation.

3.2 Re-evaluation of IP and Resistivity data

3.2.1 Introduction

This work is party concerned with reprocessing and reinterpretation of the existing geophysical data acquired between the years 1976 and 1977 by Ethiopian Institute of Geological Survey (E.I.G.S.) UN Mineral Exploration Program in Ethiopia. Preliminary

desk study, before the actual field work began, was carried out to review literature and coordinate the existing IP/Resistivity data in order to identify and localize the target areas. These areas should then be further tested in detail by appropriate geophysical methods. An attempt was also made to obtain some idea about the magnetic properties of the area from the 1:10,000 scale magnetic contour map prepared by the same Institute and also to use geological and geochemical maps.

In the re-evaluation program, a total of 14 profiles of IP/Resistivity data are reprocessed, regridded, smoothed and plotted in variety of forms, and reinterpreted.

3.2.2 Elements of IP/Resistivity surveying

3.2.2.1 The IP method

Though early work by Schlumberger to describe the chemical basis of the IP phenomenon dated back to 1920 (Keller et al, 1979), IP as a prospecting method was first put to practical use about 30 years after this early effort (Scott et al, 1969). The phenomenon of induced polarization is extremely complex and has not yet been completely understood. Nevertheless, certain facts have been established as a result of quite large numbers of research works carried out in the field of electrochemistry and most notably in geophysics. Particularly, after Bleil , who rescued the method from oblivion, a great deal of theoretical and experimental research works have been done to study the different facet of IP phenomenon and factors influencing the polarization of minerals and rocks. As a result, many great advancements in instrumentation, interpretation, and in dealing with the noise problem caused by electromagnetic coupling.

Possibly the most inspiring improvements have been made in instrumentation with the advent of microprocessors. High quality IP data are nowadays efficiently collected using microprocessor controlled multichannel receivers. Data processing and interpretation are routinely accomplished with the aid of computer programs.

Since silicates and carbonates that mainly constitute most rocks in the ground are classed as insulators, the electric current in the ground is chiefly controlled by conductors and the electrolytes present in the pores of rocks. However, when clay and conductive minerals are present dispersed in the electrolyte host medium, a system of fluid-conductor interface is formed in the contact between the ionically conducting fluid and the solid mineral grain in which the conduction mechanism is basically electronic in nature. At these interfaces either of the following two phenomena can occur: If the mineral is conductive, charge transfer across the interface can take place only when electrochemical reaction such as oxidation-reduction occurs, or when an external electric field is applied the transport of cations and anions in the interphase region near the metal- electrolyte interface will involve both drift and diffusion flux density. The flow of ions to or from the conductor-electrolyte interface causes an excess or deficit of inactive ions to accumulate, since the metal is neither a source nor a sink for these ions. These inactive ions are loosely held to the metallic particles by image forces, and concentration gradients build up which oppose the migration of these ions due to electric fields. Besides the inactive anions and cations, a minor concentration of active cations is assumed to exist in the electrolytic medium and the electric fields at the electrolyte-metal interface cause these to engage in electrochemical reactions making possible charge transfer across the interface (Wong, 1979). If the mineral grain has a net structural charge imbalance, on the other hand,

excess ions congregate in the solution near the mineral surface. This owes its origin to the presence of clay particles. The surface of clay particles are commonly negatively charged and thus adsorb an excess of positive ions in the surface of a clay aggregate to form what is often referred as the **double layer** that is comprised of the fixed negative charge on the clay particles and the mobile positive charge in this solution layer adjacent to the grain.

Polarization is therefore attributed to either the presence of interfaces between zones of electronic and ionic conduction which is referred to as **electrode polarization** or to the presence of zones of unequal ionic transport properties that gave rise to **membrane polarization**. Sulfide minerals and graphites are sources of electrode polarization; while clays and ziolites are sources of membrane polarization (Hearst et al, 1985).

Thus, the electrolyte-conductor interface has an impedance that is dependent on the electrochemical reactions and on the transport of reactive ions to feed these reactions.
The electrochemical analysis of electrode impedance in planar geometry in ore bodies have been discussed by many authors in the field of electrochemistry and geophysics. It is found that the impedance of planar metallic electrodes immersed in electrolytic solution are frequency dependent or dispersive. For cases in which the rates of the charge transfer reactions at the metal-electrolyte interface are determined by the diffusion of active ionic species to the reaction sites at the interface, the dispersive impedance involve a component whose magnitude is proportional to the inverse square root of frequency (Warburg impedance or diffusion impedance.). However, because this geometry is unrealistic for the case of ores containing disseminated mineralization, the results are not directly applicable to the IP effect encountered in exploration geophysics.

J. Wang (1979) has considered a spherical conducting sphere to study the impedance mechanism on a better physical model and based on electrochemical principle and electrical potential theory. Despite the simplification, a number of interesting and important results are obtained along with emphasizing the low frequency dispersion in the resistivity. It is found that the conductivity and resistivity spectra calculated from this electrochemical model do account very much for the experimental data obtained from laboratory measurements on synthetic metalliferous ores.

In his theory of a single electronically conducting spherical particle residing in an electrolytically conducting continuum, Wang has established a formula for the electric dipole moment associated with the sphere that consists of a constant term and a frequency dependent part. The constant term represents the dipole moment of a perfectly conducting sphere in the uniform external field, whereas the frequency dependent contribution is due to electronic charge in the metallic sphere that are images of the ionic space charge on the electrolyte side of the phase boundary. He describes the similarity to the classical two plate capacitor as "The two layers of charge, one on each side of the metal-electrolyte interface, can be considered to be similar to the two plates of capacitor. However, because of charge transfer reactions involving minor constituents in the ionic space charge, the double layers of charge behave more like an imperfect capacitor which leaks change. Moreover, the charging to the interface is determined by the mass transport of ions to replace the leaked charge and supply active ions for the charge transfer reaction".

grains. A number of findings including the following characteristics common to all specimen were reported:

1. The chargeability is nearly constant between current densities of 0.01 and 0.1 μA/cm.sq.
2. The chargeability decreases by about 20 percent per decade increase in current density between 1 and 100 microA/cm.sq.
3. There is no indication in any of the curves that chargeability will not continue to decrease with increase in current density, and
4. The background effect was indistinguishable in its decay form from the IP effect due to the sulfides.

The interrelation of chargeability, resistivity, porosity, sulfide content and sulfide grain size for low current density is investigated by averaging over identical specimen with a given sulphide content and grain size. It becomes obvious that sulfide content and the grain size are the controlling factors in determining the chargeability of the specimens, with the fine grains being more polarizable than the large grains, and chargeability are approximately proportional to sulphide content. However, no clear correlation exists between chargeability and resistivity or porosity. For current density greater than 1μA/cm.sq chargeability decreases as current density increases, regardless of the specimen parameters. However, individual decay curves show no obvious change in shape or rate of decay with increasing current density. The effect is apparent only as a change in amplitude. The background chargeability observed in quartz-loaded specimen had the same dependence on current density as the sulphide particle polarization. The background chargeability increases with increasing quartz grain size. This is opposite to the relationship for metallic particles.

shape or rate of decay with increasing current density. The effect is apparent only as a change in amplitude. The background chargeability observed in quartz-loaded specimen had the same dependence on current density as the sulphide particle polarization. The background chargeability increases with increasing quartz grain size. This is opposite to the relationship for metallic particles.

The concept of chargeability as postulated by Seigel involves the monitoring of the decaying voltage after the current is switched off (Keary et al, 1984). The theoretical chargeability M is thus defined as the area beneath the decay curve over a certain time interval normalized by the steady-state potential difference. That is

$$M = \frac{1}{Vc}\int_{t1}^{t2} Vp(t)\partial t$$

where Vc is the steady state voltage during the current flow, and Vp(t) is the polarization voltage over a certain time interval (t_2-t_1).

3.2.2.2 Resistivity method

The feasibility of using resistivity method in base metal exploration is based on the well-marked resistivity contract between the ore bearing formation and the host rock. Most rock forming minerals are insulators and, as rocks are not formed of minerals alone, their resistivities are generally determined by the porosity of the rock, mineralization of the pore-electrolyte, temperature, pressure and to some extent by the mineralogical composition of the rocks. However, in most conductive minerals, graphite and notably base metal sulphides except sphalerite, conduction takes place by the flow of mobile electrons and such minerals are characterized by low resistivity. The resistivity of ore formation is thereby a function of both the amounts of conductive minerals present and

the mode in which they are distributed in the ore. When they form a continuous interconnected network so that there should be no discontinuity in the current flow, the rock resistivity will be reduced to a very low value. Thus, while massive volcanic associated sulphide ores or hydrothermal and skarn deposit types have low resistivity; porphyry copper ores, cupriferous sand stones and impregnation ores, where the individual grains of conductive minerals are not in contact with each other, aquire relatively higher resistivity and become less amenable to resistivity prospecting or most of geophysical methods (Kuzvart et al, 1979).

The simplest approach in dealing with apparent resistivity measurement in resistivity prospecting is to consider the case of a homogeneous isotropic earth model. If the current electrodes are designated by A and B , and the potential electrodes by M and N, the equation for the apparent resistivity in homogeneous isotropic earth for this four electrode systems is given by

$$\rho_a = \frac{2\Pi}{\frac{1}{AM} - \frac{1}{BM} - \frac{1}{AN} + \frac{1}{BN}}\left(\frac{Um - Un}{I}\right)$$

$$= K\frac{\Delta U}{I}$$

where AM, AN, BM, and BN are distances between the current and potential electrodes, Um and Un are the electrical potentials at points M and N respectively, I is the electrical current, ρ_a is the apparent resistivity and K is the Geometric Factor (Keller et al, 1979).

In the polar dipole-dipole system, when the separation between both pairs of electrodes is the same, say 'a', and the distance between the two innermost electrodes is 'na' the expression for the geometric factor will be

$$K = \frac{2\Pi}{\frac{1}{na} - \frac{1}{a-na} - \frac{1}{a+na} + \frac{1}{2a+na}}$$

$$= \pi n(n+1)(n+2)a$$

and hence, for the apparent resistivity, we have

$$\rho a = \pi n(n+1)(n+2)a\left(\frac{\Delta U}{I}\right)$$

3.3 Data acquisition, processing and interpretation

3.3.1 Survey lay-out and field procedure

The plan map showing positions of the profiles, drill holes and the gossan zone is given in Fig. 4. Though a total of 14 profiles are incorporated in the re-evaluation work, only 9 profiles lying in Katta II area are indicated in the figure. Measurements for both chargeability and apparent resistivity were obtained by using the polar dipole–dipole electrode configuration with a fixed electrode spacing of 100m and dipole spacing 'n' restricted in the range of 1 to 8. For rapid sequential acquisition of multiple spacing data and for reducing the labor of moving the current electrode and other survey instruments, for each increased spacing, five current electrode arrays at a fixed inter-electrode spacing of 100m have been employed. This arrangement permits the electrodes to be connected in various dipole-dipole configurations so do the dipole spacing 'n' to vary from 1 to 8. Current was generated by a 2.5 kw IPC-7 Scintrex transmitter, and IP/Resistivity was

measured by an IPR-8 Scintrex receiver. Only three time integral slices were taken and normalized automatically by the instrument to obtain the chargeability at each station. The three segments (slices) have 2-second total integration time, and the DC-pulse duration and the current–off time were both kept at two seconds (Kuznetsov).

It has been indicated that intensive and varying earth noise, externally unfavorable grounding condition, insufficient polarizing current was a serious problem (Ibid). In order to alleviate some of these problems, two electrode pits of about 1.8 by 0.8 by 0.5 meters were dug across the lines at each electrode site and filled with corrosion resistant wire mesh screen or aluminum foil and water with common salt to provide effective grounding, and to enable to reduce the current electrode resistance. Porous pots prepared from water with a dilute copper sulphate solution were used as potential electrodes.

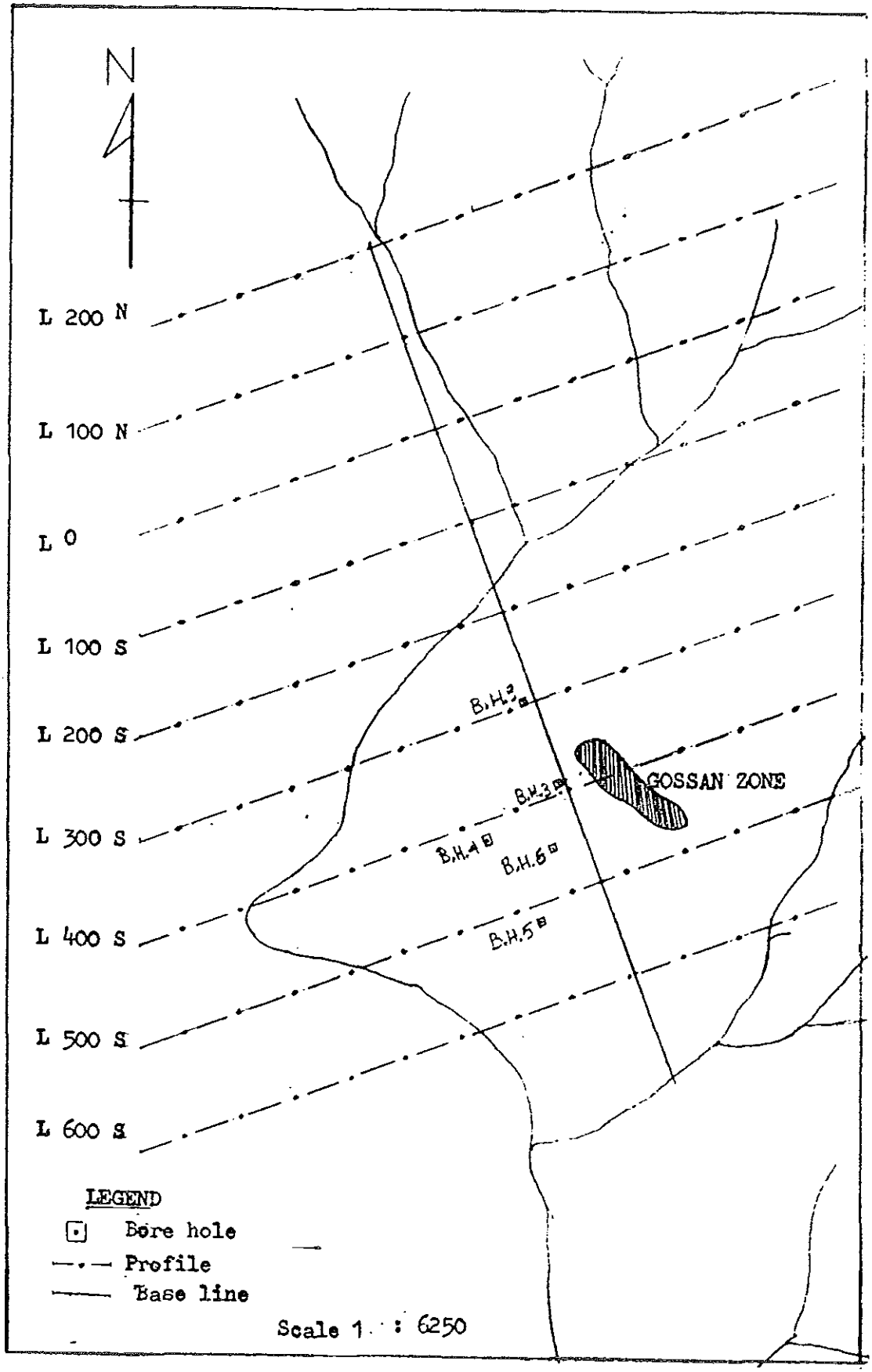

Fig. 4 Survey Lay-out of Katta II Area

3.3.2 Data processing

Both the IP and resistivity data are arranged in 2-dimensional 'pseudosection' and as multilevel plan map to display the horizontal and vertical variations in chargeability and apparent resistively. The conventional method introduced by Hallof is applied to produce the contours. According to this method, each values of the chargeability and apparent resistivity measured for each set of electrode positions are plotted at the intersection of the grid lines drawn through the two dipole centers. Each data point, assigned to a specific value of 'n', is by assumption related to a given effective depth of investigation. The result is thereby a qualitative picture of both vertical and horizontal variations in chargeability and apparent resistivity. Surface contour for each 'n' level is also constructed to examine the lateral variation, though this procedure introduces wrong information in the plan map because the most anomalous values usually do not overlie the causative body. To overcome this limitation, Fraser introduced a reduction technique for presentation of multilevel dipole–dipole data in a single surface contour that reflects all levels of the pseudosection (Fraser, 1981). According to his view the technique provides a quantitative picture of IP anomalies in their background or regional settings. The technique has been applied to contour the IP/Resistivity data in plan map.

The principle of this reduction technique is simple and straight forward. A simple averaging filter of triangular shape is first applied to each level. In this process, the first level is unaffected, the average of two adjacent values is taken for the second level, three for the third level, etc. These average values, termed the "intermediate output," are then averaged again to yield the final output.

3.3.3: Interpretation

The broad features of the observed chargeability and apparent resistivity space from pseudosections and different level plan maps may be summarized as follows:

1. The possible anomalous zone is clearly delimited by gently dipping clusters of contours in two sides, one from east and the other form west of the baseline. These outward dipping contours are nearly symmetrical and plainly marked in most of the chargeability pseudosections.
2. These features are suppressed due to insufficient data set in profiles 100N, 300S, 700S, 900S, and 1100S
3. It is to be noted that the concentrated contours are restricted in extent; an indication for abrupt change in electrical properties.
4. They also fail to form closed contours at the top. This together with the range of 'n' levels most of maximum responses are localized indicates the shallower depth of the anomalous zone.
5. The chargeability response outside this zone on either of the sides falls off rapidly and maintains a minimum of 3 ms to 6 ms that represents the background effect.
6. As shown on the resistivity pseudosection in Fig. 5, contours of very low resistivity correspond to the high chargeability zone.
7. Outside this zone due east, a sharp discontinuity appears marked by high gradient contours that distinguish the anomalous zone from highly resistive body. This is seen to best effect between the profiles 200N, and 200S. On the other hand, an effect from relatively deeper resistive body west of the anomalous zone starts to appear on profile 200S, then again on profile 400S and become conspicuous in the successive ones. This has been manifested through dome shaped contours of high resistivity at

the second or third n levels. In general, buried causative bodies fail to show identifiable features for small values of n depending on their depth of burial.

8. The above situation has been taken to indicate the possible synformal depression separating two highly resistive masses.
9. A more serious problem is an excellent IP/Resistivity response of graphite and pyrite disseminated within a wide zone of phyllite and schist, and thick weathered overburden of schist that have been altered almost to clay (Wahi, 1982). It is extremely difficult, if not impossible, to differentiate these causative bodies from sulphide minerals and hinder accurate interpretation on the result of the IP and Resistivity observations.

When going on from a bird's eye view to a more detailed consideration, the contour maps reveal that most of the IP/Resistivity features belonging to profile 200N are also inherent as common features to many of the remaining profiles. So, profile 200N is chosen to show the background level. The term background level as used here may not mean an order of 16 ms chargeability and as low resistivity as 200 Ohm-m characterize the host rock. The term under discussion is used to mean that profile 200N would serve as a reference in order to delineate the most prominent anomalous zones. The plots shown in Fig.5(a) and Fig.6(a) are respectively apparent resistivity and chargeability pseudosections obtained for profile 200N that ran over -650 meters to 250 meters. The apparent resistivity and chargeability responses are variable from 200 Ohm-m to 2000 Ohm-m and 3 ms to 6 ms, respectively. To the west of the base line, both the resistivity and chargeability show variations over short distances. In view of the disseminated nature of mineralization and highly weathered overburden condition reported in the area, the

variation is presumably due to the presence of graphite, clayey formation and dispersed mineralization associated with quartzite, greenschist, and phyllites, typical of the survey area. A fairly good correlation of an increase in apparent resistivity with decrease in chargeability and vice-versa is observed on their corresponding locations. To the east of the base line, on the other hand, the resistivity gradient remarkably increases and forms closed contours at the top and open at the bottom, except in the inner most ones. The area is correlated by low level chargeability effect in the IP pseudosection as shown in the Fig. 6(a). The dipole- dipole pseudosection along traverse 200N is thus characterized by low resistivity and high chargeablity zone between coordinates -650 m and 0 flanked on both sides by high resistivity correlated with low chargeability zone. The resistivity high is diagnostic of near surface basement rock, while the low resistivity zone with high chargeability response may be attributed to a synformal depression overlain by weathered metasedimentary rocks comprising graphite schist.

Apparent resistivity and chargeability pseudosections for the fourteen profiles are respectively plotted on Fig. 5 and Fig. 6. The plan map for the 7 level pseudosections is given in Fig. 7. The basement, mentioned with profile 200N, seems to follow a definite direction and appears prominent up to profile 400S, except a discontinuity near by profile 100S. There looks to exist a correlation between this body and the metagranodiorite indicated on the geological map of Fig. 3 of the Katta area. According to Soukhoroukov, these metavolcanic rocks, including the metadiorite, are the oldest rocks in the area and are considered to be the most deeply eroded strata.

It will be interesting enough to note a striking correlation of Fig. 3 with the resistivity plan map fig. 7 in delineating the East-West traversing shear zone nearby profile 100S. The zone may be categorized on Soukhoroukov's classification, under the 60^0-70^0 NE trending fissures. The shear zone and the southward continuation of the resistive body are plainly shown in the resistivity plan maps. The nature of the IP response in this zone, however, remains smooth and unchanged. The reasons for the IP measurement missing this narrow fissure zone may be interpreted as either because of the complete absence of polarizing bodies or due to large dipole spacing used. But the latter is rather convincing than the former, since the low resistivity trace imprinted at different levels of the resistivity plan map indirectly imply the presence of conductive bodies which from the geological and geochemical point of view of the area, are either sulfide associated mineral areas or graphite and clay particles composed of phyllites and schists. If this is the reason, an inference on the resolving power of the two geophysical methods in detecting narrow conducting bodies can be made within the frame work of the dipole configuration and identical electrode spacing used in the survey.

Chargeability pseudosections for the 14-profiles are plotted on fig. 6. Peak values are recorded on all profiles; the prominent peaks in the range of 27-42 ms all lying between lines 100S and 700S. The anomaly on profile 400S is in good agreement with the geochemical result and ore mineralization established in Kate II. In this area surface gossaniferrous body with definite strike pattern of SE–NW direction is exposed 40 to 60 meters east of the base line. Geochemical sampling along this zone established copper values of as high as 3200 PPM (Wahi, 1982). And from drill hole No 3 (Azimuth 50^0, Inclination–45^0, assumed coordinates 392S/ 2E relative to the geophysical grid) a value of

2.86% Cu across 15.24m was obtained (Ball, 1982). This borehole is the closest of all the boreholes drilled in Katta II to the surface gossan (see fig. 4).

The IP pseudosection and plan map results together show at least five pronounced anomalous zones within Katta II locality. One IP anomaly zone that lies mainly along profile 200S, about 105m east of the base line, extends up to profile 100S. The anomalous pattern show a peak value of 30ms at upper most level (shallower depth) and rapidly decreases to the background value at fourth level plan map. This zone is also very well correlated with low apparent resistivity value of 100 Ohm-m at shallower depth. As detail SP and IP/Resistivity Survey results, carried out later on, show peak SP anomalous value of more than -300 mv and good IP response corroborated by low resistivity value is obtained over this zone. But, in view of the very high potential gradient on either side of SP peak, and subsequent confirmation obtained from the stream section, it was deduced that the source of this anomalous zone is related to lens of graphite schist (Wahi, 1982).

Along the same profile 200S another anomalous body of rather restricted lateral dimension is found around 130 m east of the base line. It is situated within the lower level plan maps and attains peak values of 24 ms in the 5^{th} and 6^{th} level. The third anomalous body is confined to shallower depth, 150m west of the base line, along profile 300S. It appears only in the third level plan map with peak value of 30 ms and has restricted dimension like the earlier case. These anomalous zones are outlined by relatively low apparent resistivity values in the range from 100 to 400 Ωm. The presence of such small pockets of ore bodies are not unusual for an area where the main mineralization is supposed to be a result of remobilization process, established at Katta II. This view is

further strengthened by the parallel and sub-parallel trend of the anomalous zones to the main mineralization that will be discussed below.

A number of evidences suggest that the gossan exposed near profile 400S and subsequent Geochemical sampling results were the reason for the relatively full-fledged exploration work and borehole drilling carried out in this zone. The remaining anomalous zones, which have a wider region of more than 200 m coverage in Katta II and which lie between profiles 400S and 600S are situated in this area of fairly large geological, geochemical, geophysical and drill hole information. Along profile 400S a two-level anomalous zone, one at shallower depth and the other at intermediate depth, lie within the interface between the near surface basement rock and the depression zone. The anomalies and the underlying topography reveal that

1. The shallower anomaly is nearly on the eadg of the resistivity relief. It is located between -250 m and -50 m stations and attains a maximum value of 42 ms.
2. The deeper anomaly is located beneath the shallower anomaly and extends downward. It attains a peak chargeability of 36 ms.
3. Likewise, the anomalies on profiles from 500S to 1100S are confined in a similar manner and attain peak values of 36, 39, 42, 36, 36, and 36 ms in their respective order.
4. There is, therefore, an obvious correlation between these parallel peak patterns and the subsurface structure in the zone.

The shallower anomaly, having limited depth extent, appears only in the second level plan map. This is anticipated to be an effect of Cu mineralization intersected by the B.H. No 3

(see Fig. 4) though field observation pertaining to the locality suggests that graphite is also present. On the other hand, the deeper anomaly is related to the zone of scattered chalcopyrite-pyrite mineralization as reported from B. H. No 4 (Ball, 1982). Thus, have they been proven viable, the anomalies in this zone could be economically attractive mineralization in terms of concentration and recovery so far classified as ore bodies. A report related to the self-potential (SP) survey has also indicated that as high SP anomaly as -230 mv of 200 m strike length, is obtained along profile 400S east of the baseline (Wahi, 1982).

To conclude, good IP responses have been obtained scattered over the anomalous zone; and the resistivity data has fairly distinguished several structural patterns. To study these zones in more detail, electromagnetic (EM) and magnetic measurements were made at shorter spacings. The results of these measurements will be outlined in the following section.

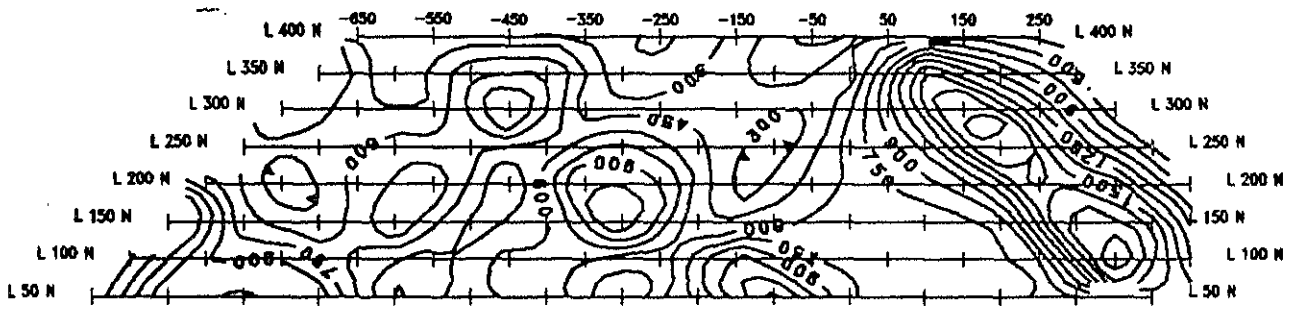

Line 200N

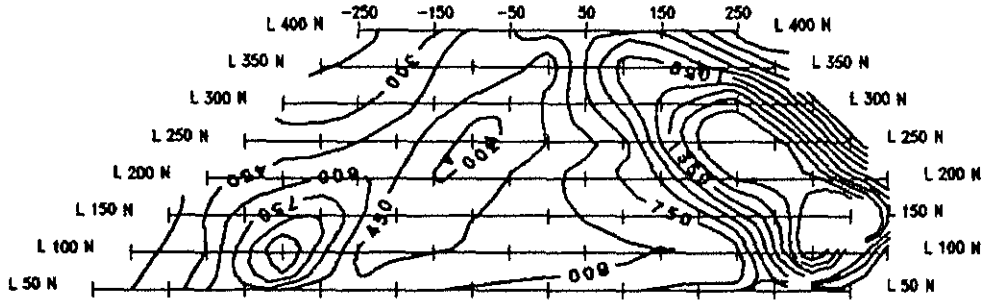

Line 100N

Fig. 5 Apparent Resistivity Pseudosection

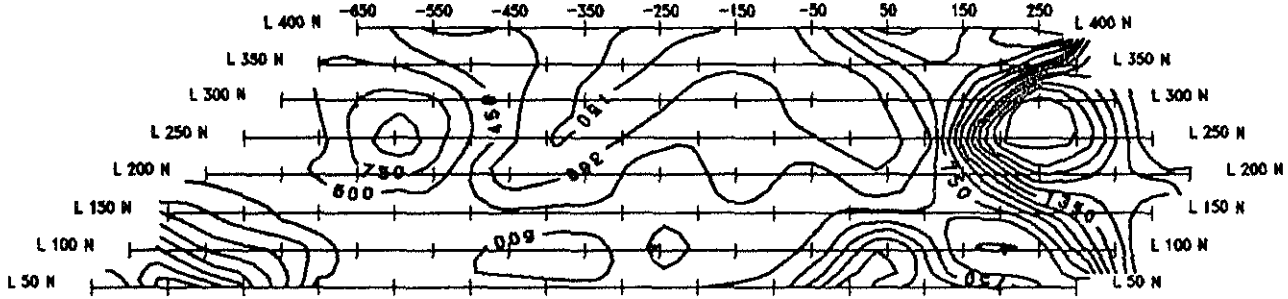

Line 0

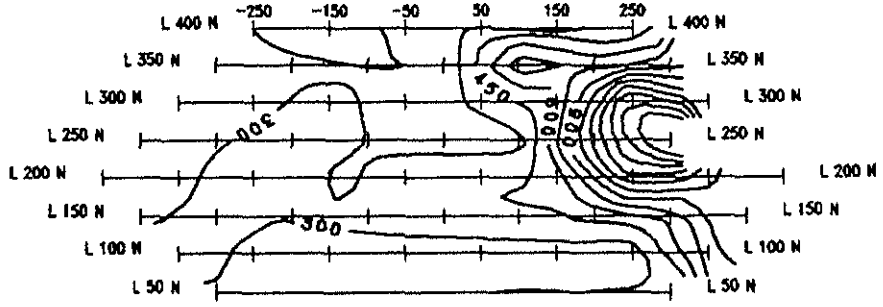

Line 100S

Fig. 5 Apparent Resistivity Pseudosection

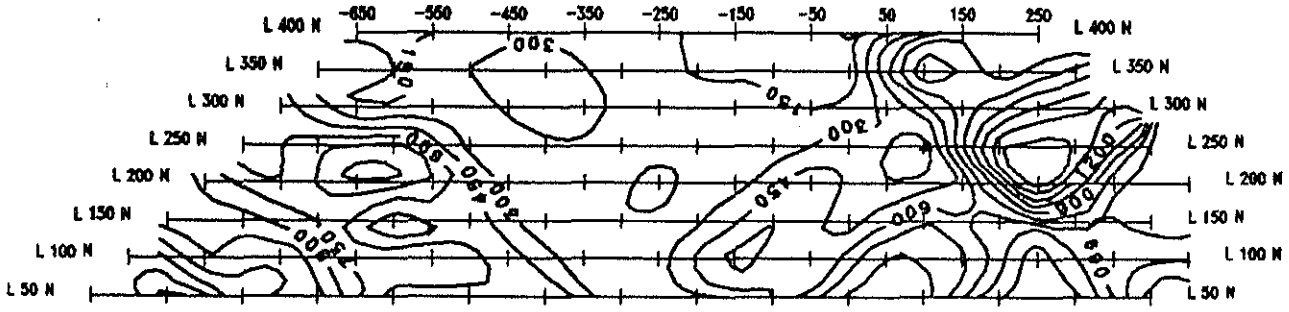

Line 200S

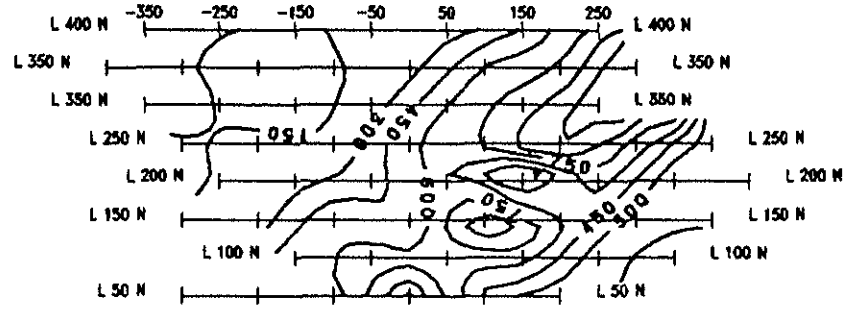

Line 300S

Fig. 5 Apparent Resistivity Pseudosection

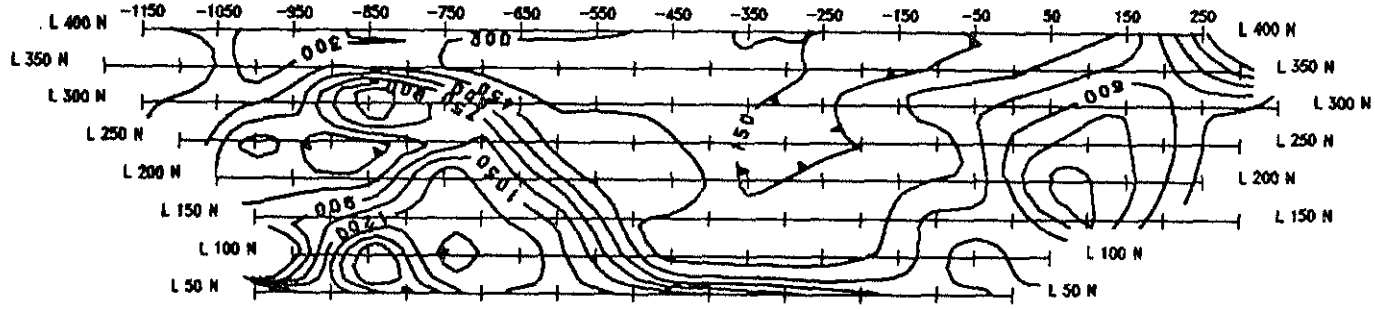

Line 400S

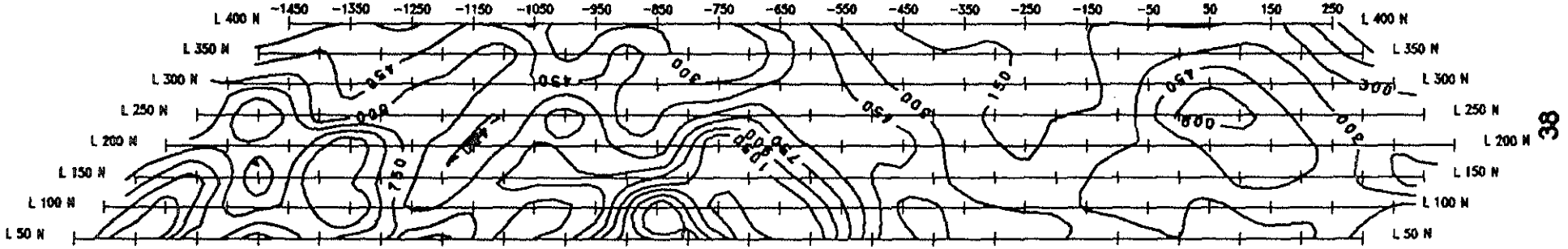

Line 500S

Fig. 5 Apparent Resistivity Pseudosection

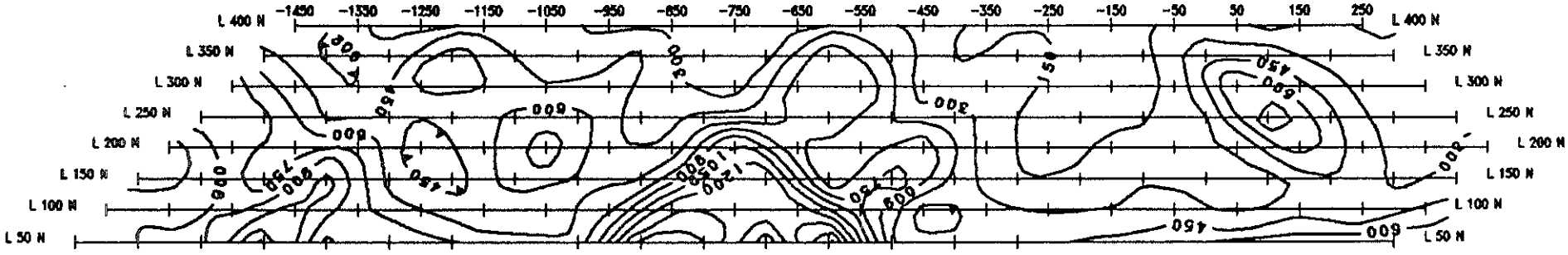

Line 600S

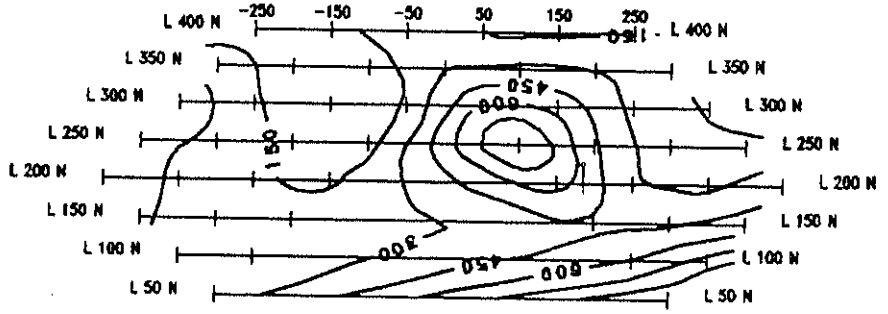

Line 700S

Fig. 5 Apparent Resistivity Pseudosection

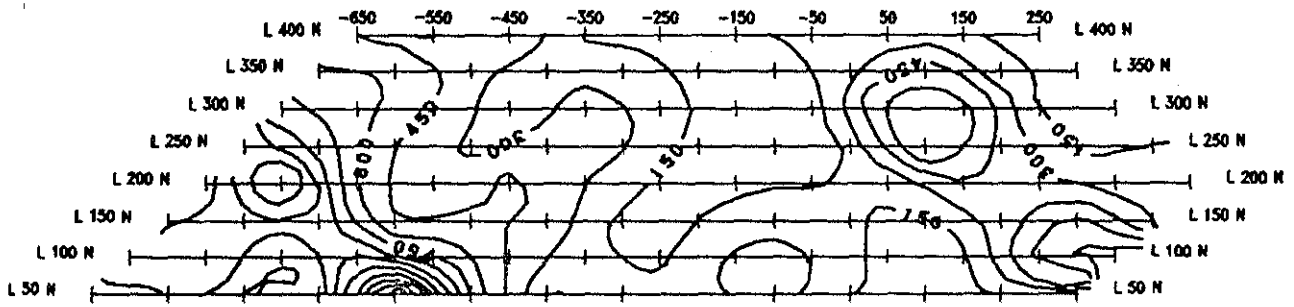

Line 800S

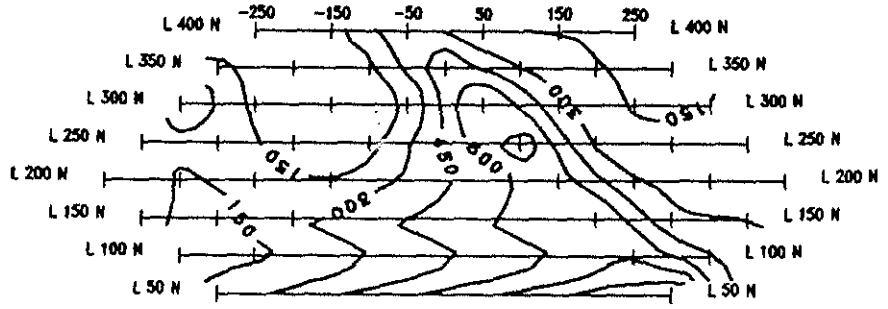

Line 900S

Fig. 5 Apparent Resistivity Pseudosection

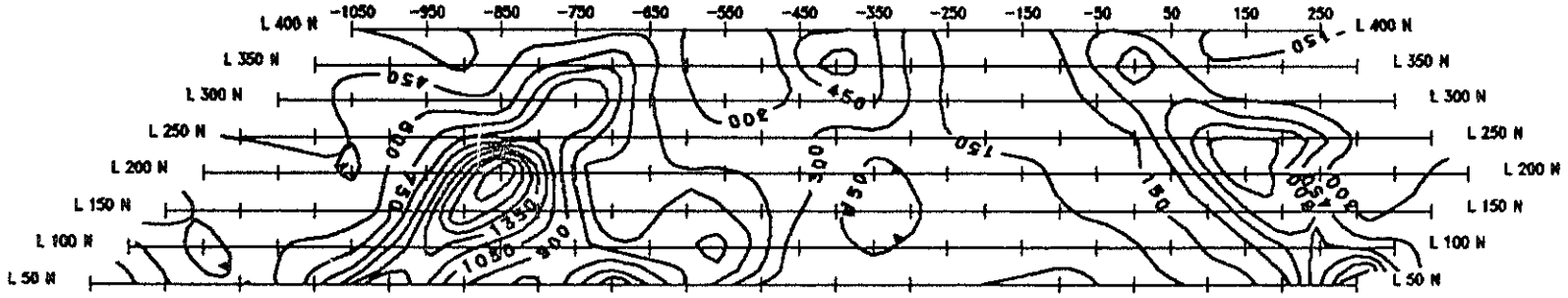

Line 1000S

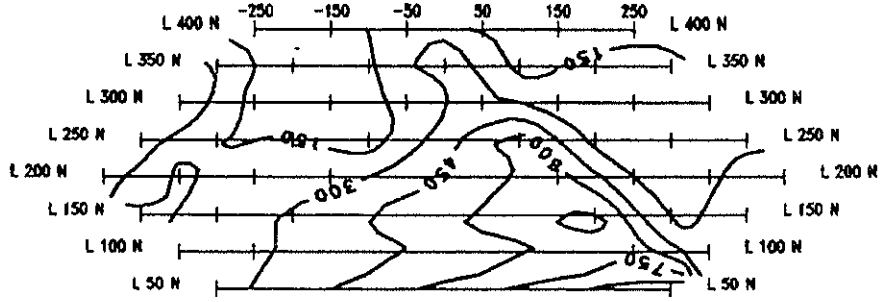

Line 1100S

Fig. 5 Apparent Resistivity Pseudosection

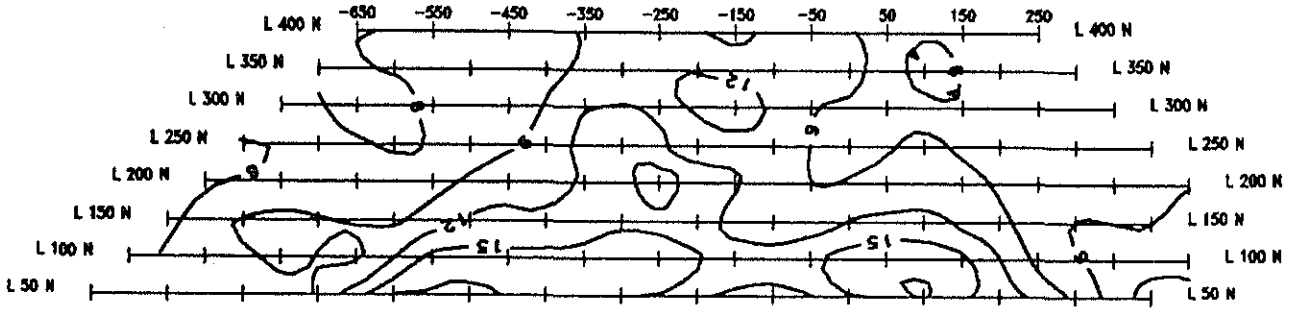

Line 200N

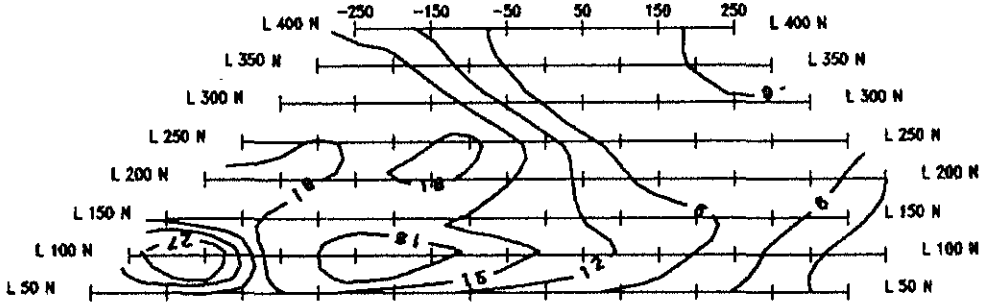

Line 100N

Fig. 6 Chargeability Pseudosection

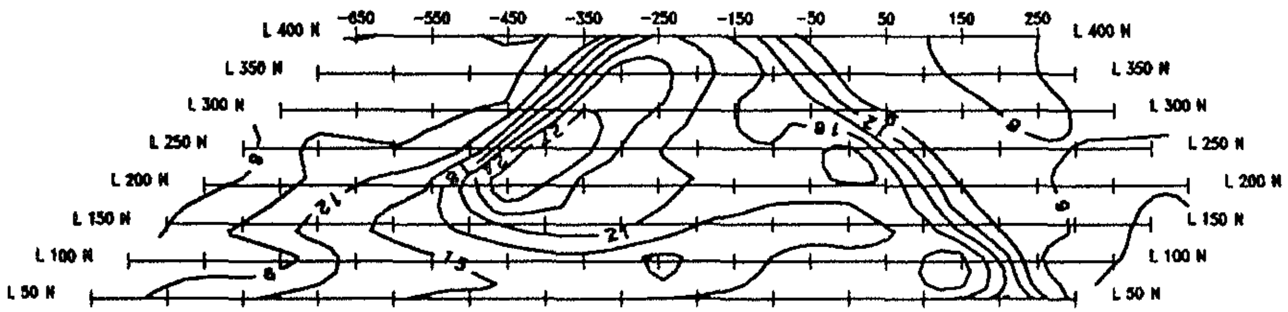

Line 0

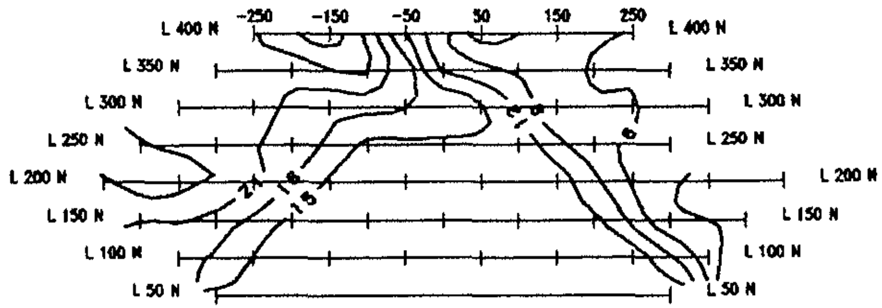

Line 100S

Fig. 6 Chargeability Pseudosection

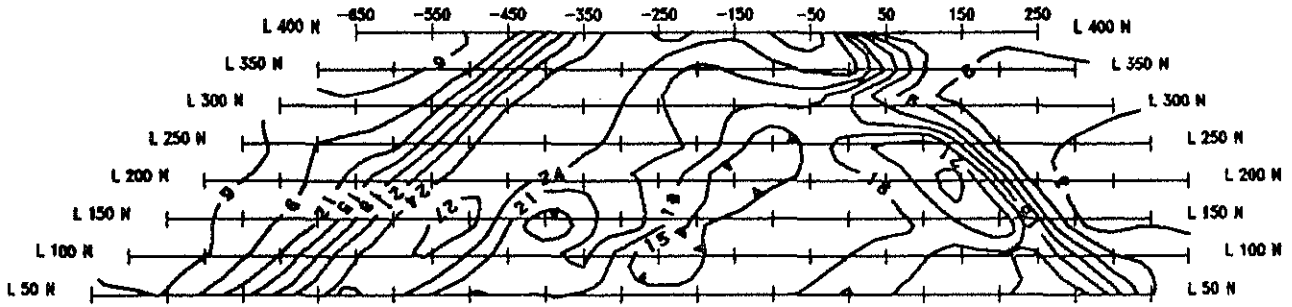

Line 200S

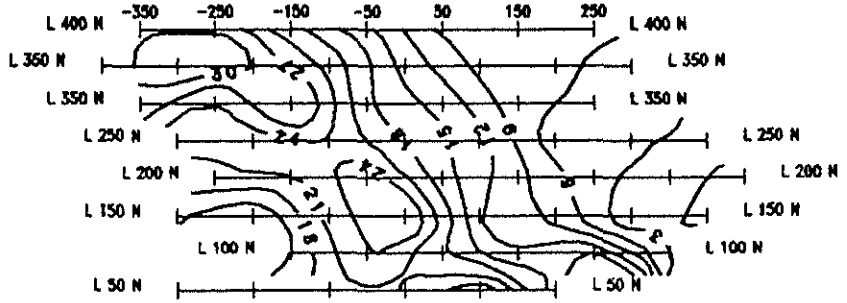

Line 300S

Fig. 6 Chargeability Pseudosection

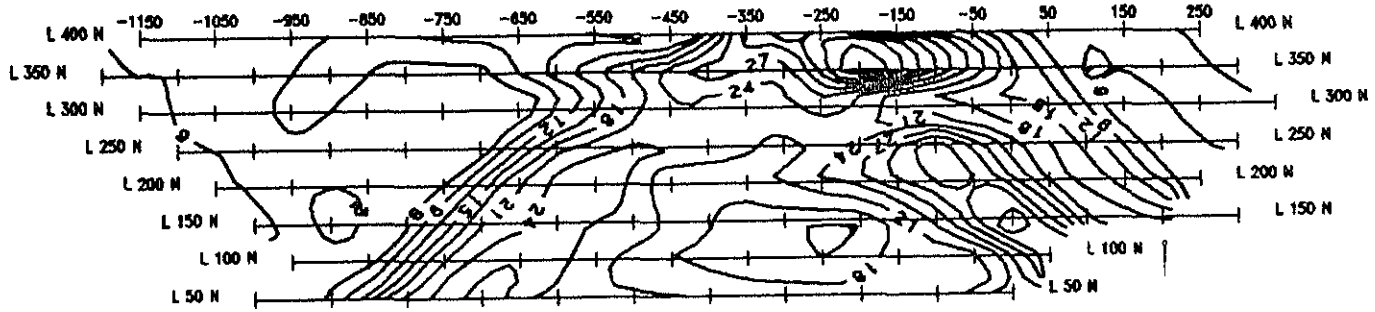

Line 400S

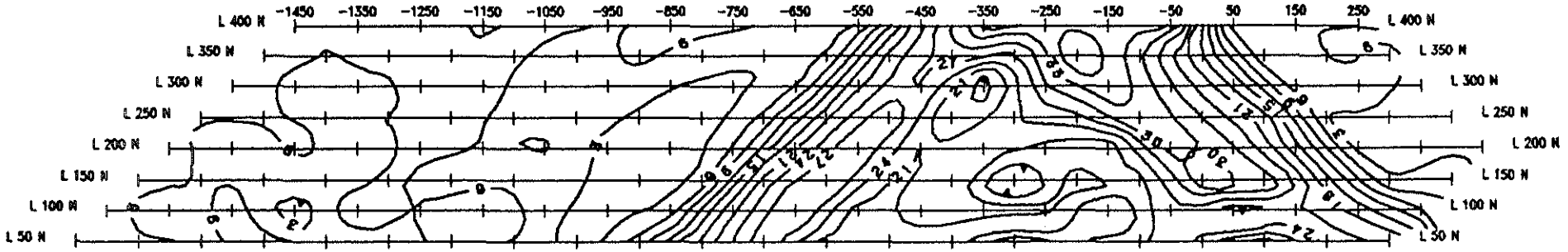

Line 500S

Fig. 6 Chargeability Pseudosection

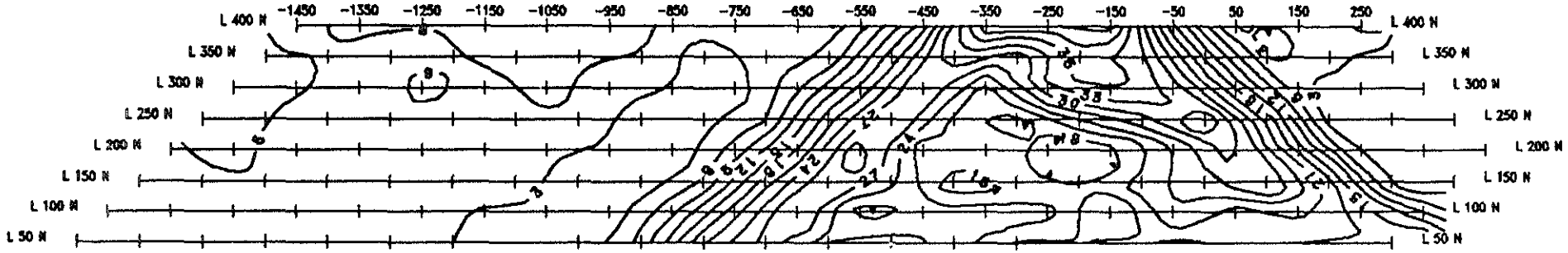

Line 600S

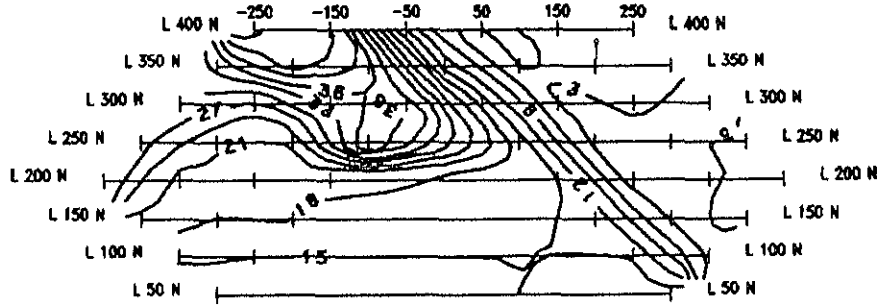

Line 700S

Fig. 6 Chargeability Pseudosection

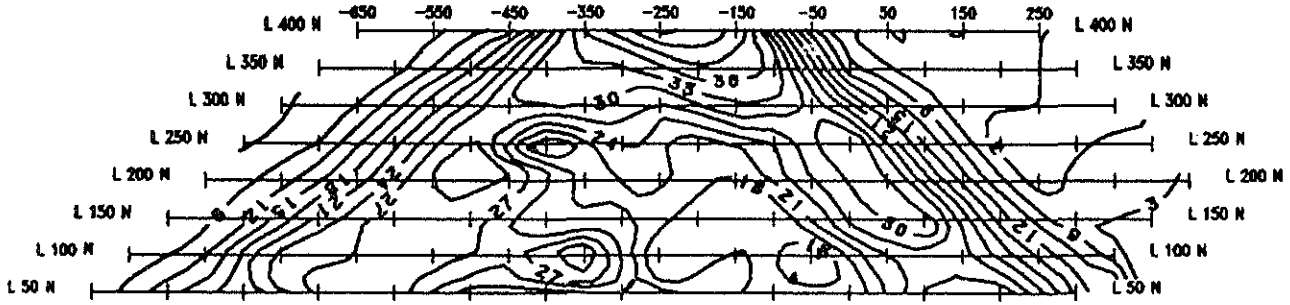

Line 800S

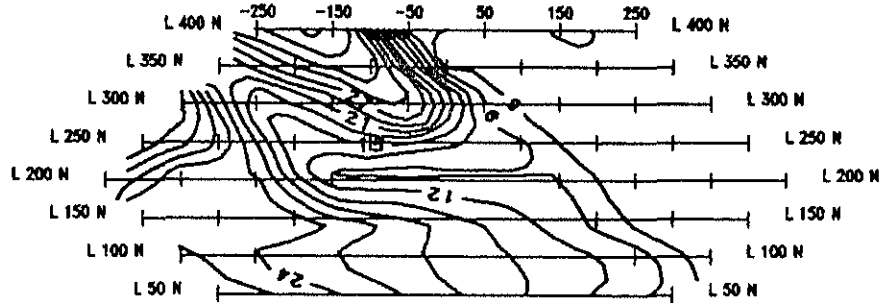

Line 900S

Fig. 6 Chargeability Pseudosection

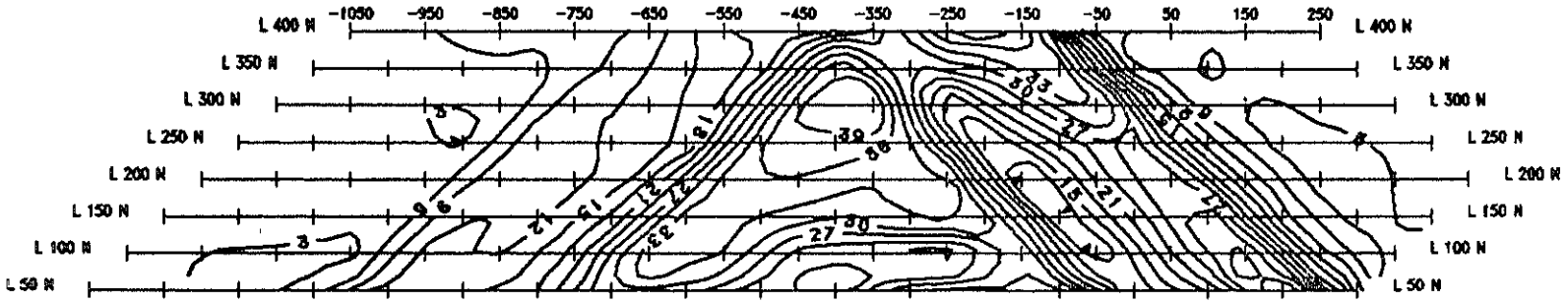

Line 1000S

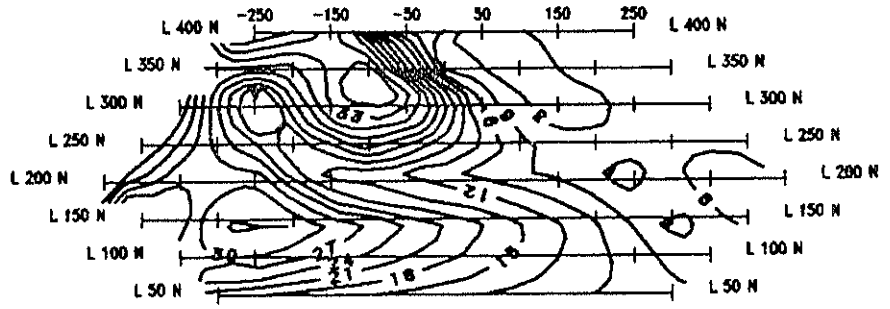

Line 1100S

Fig. 6 Chargeability Pseudosection

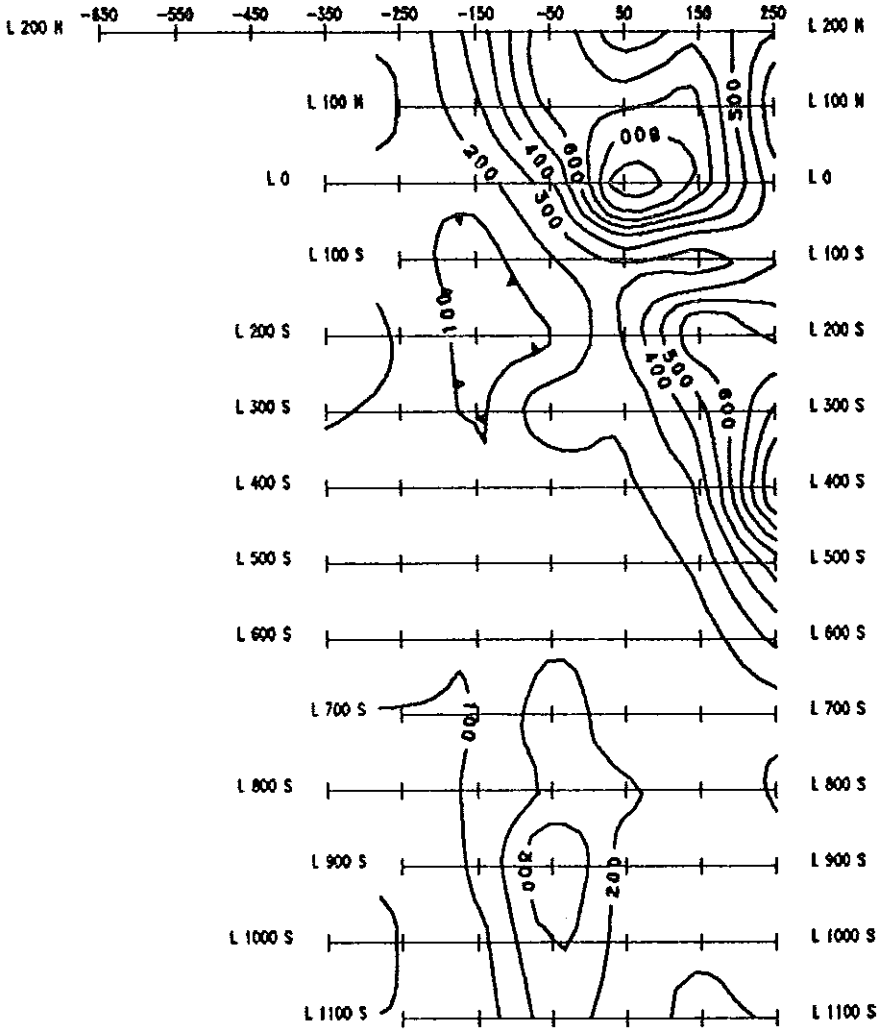

Fig. 7 Apparent Resistivity Plan Map, n=1

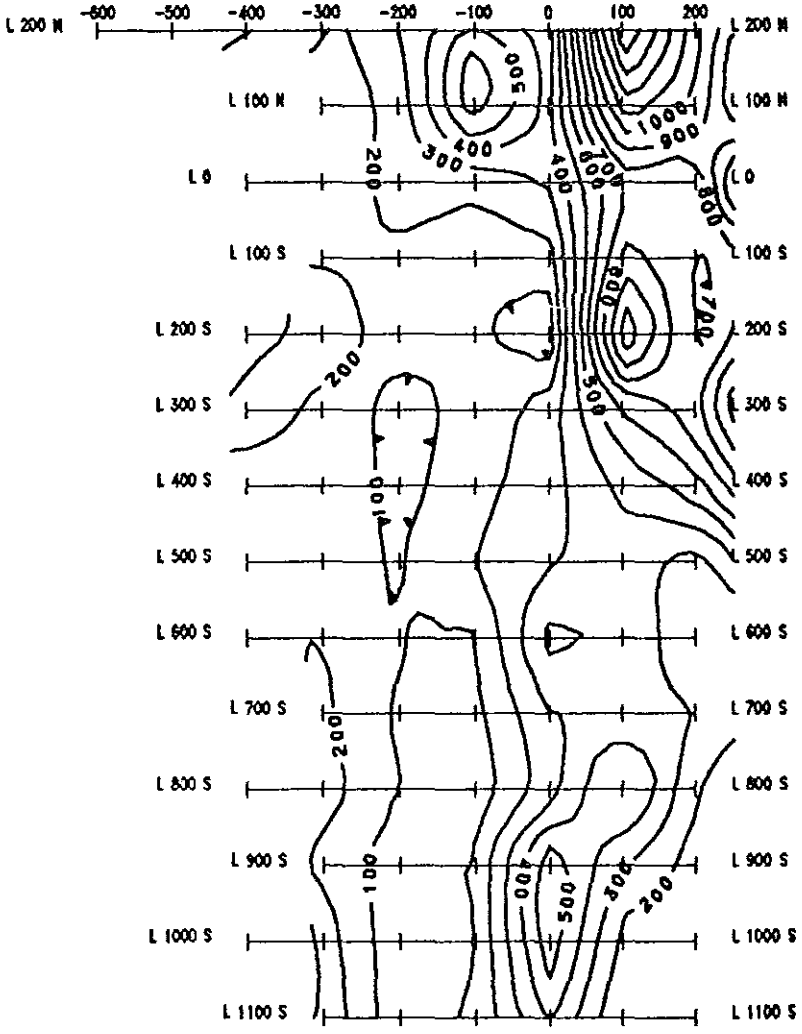

Fig. 7 Apparent Resistivity Plan Map, n=2

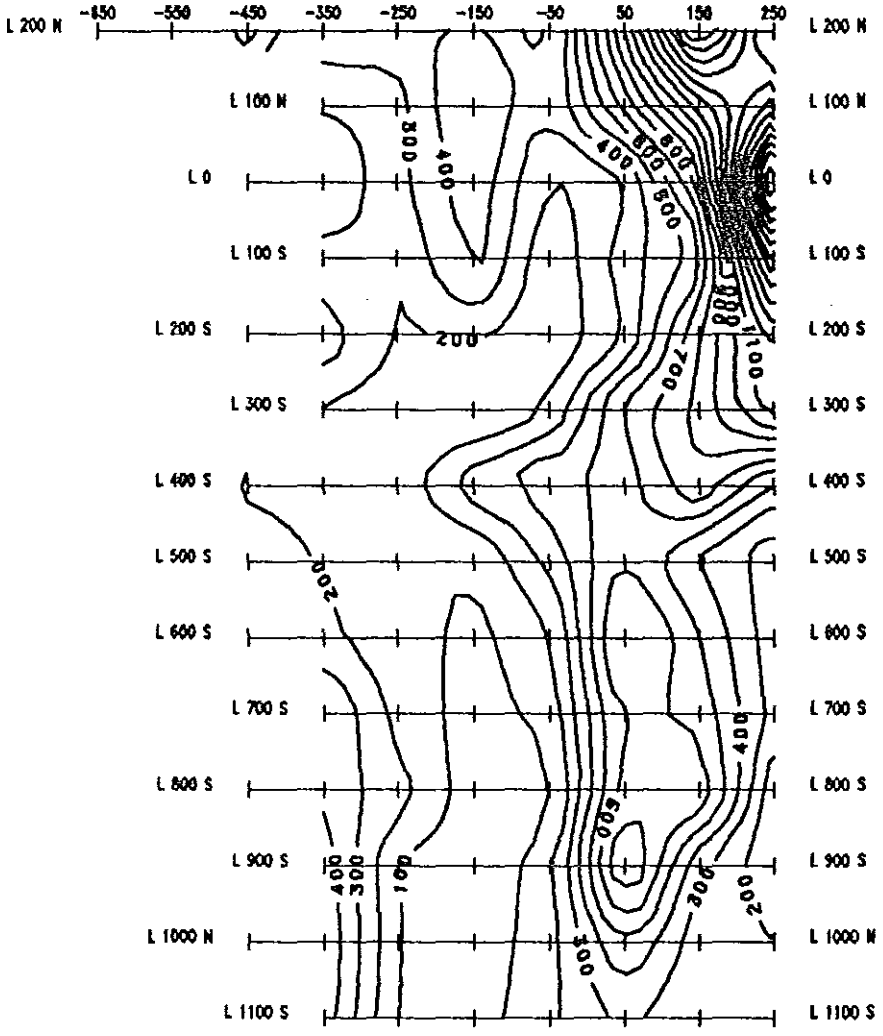

Fig. 7 Apparent Resistivity Plan Map, n=3

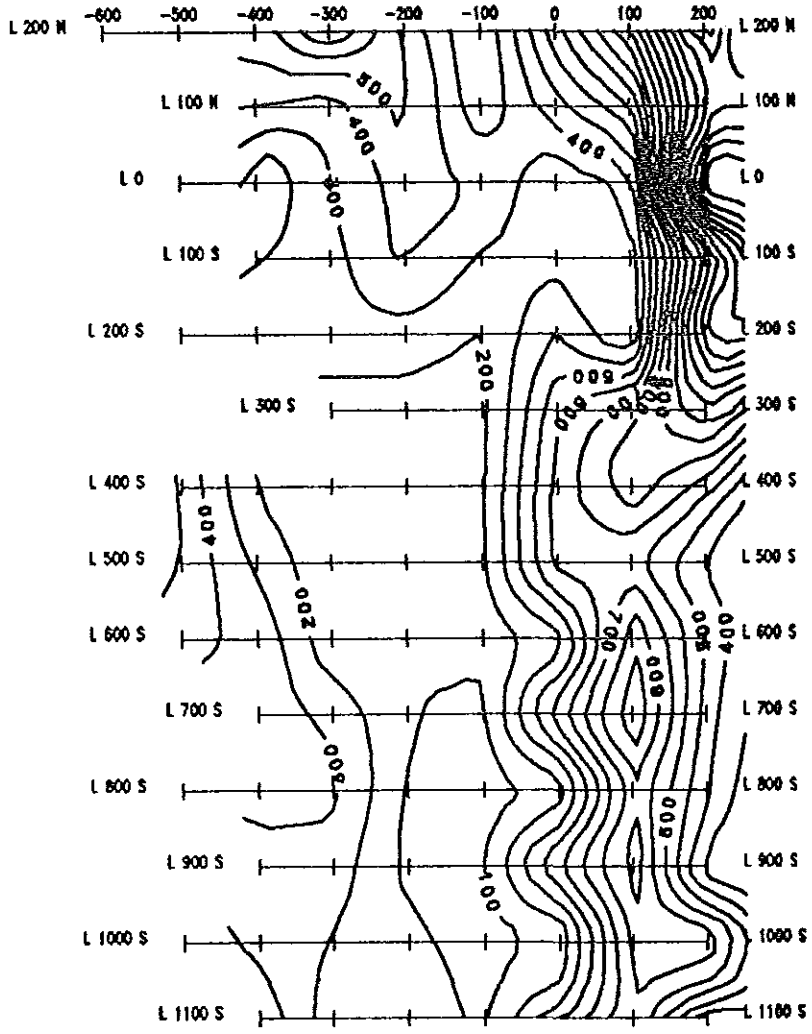

Fig. 7 Apparent Resistivity Plan Map, n=4

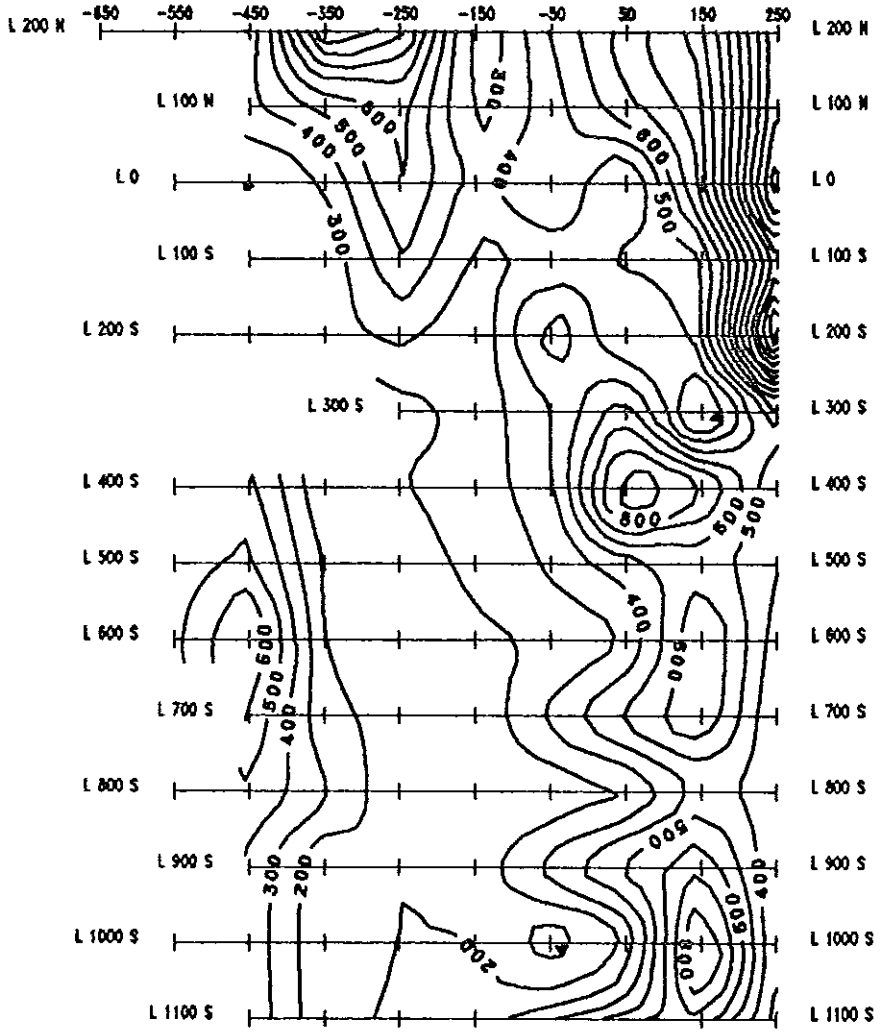

Fig. 7 Apparent Resistivity Plan Map, n=5

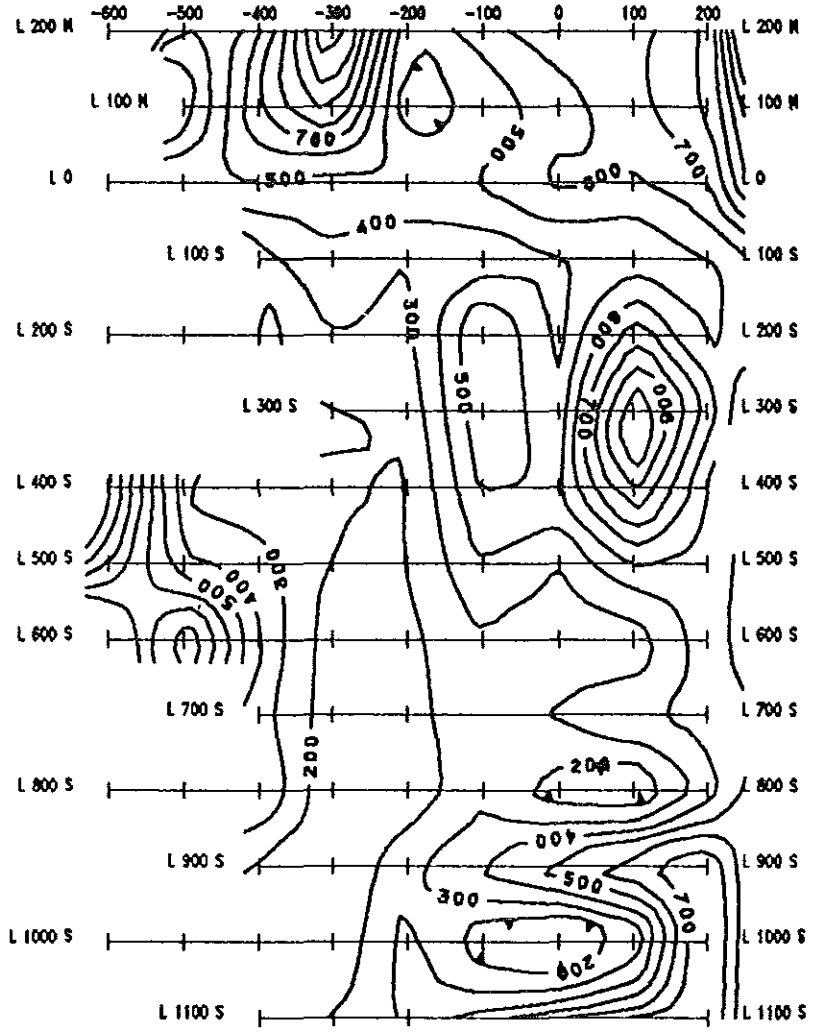

Fig. 7 Apparent Resistivity Plan Map, n=6

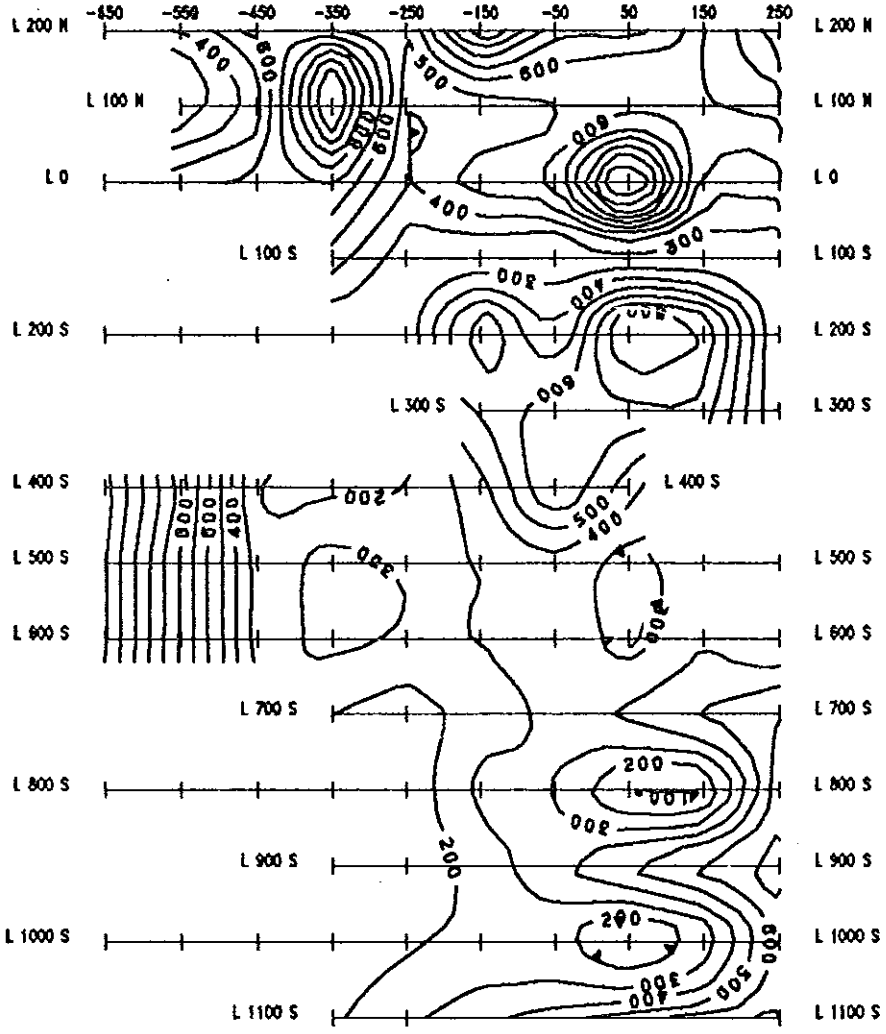

Fig. 7 Apparent Resistivity Plan Map, n=7

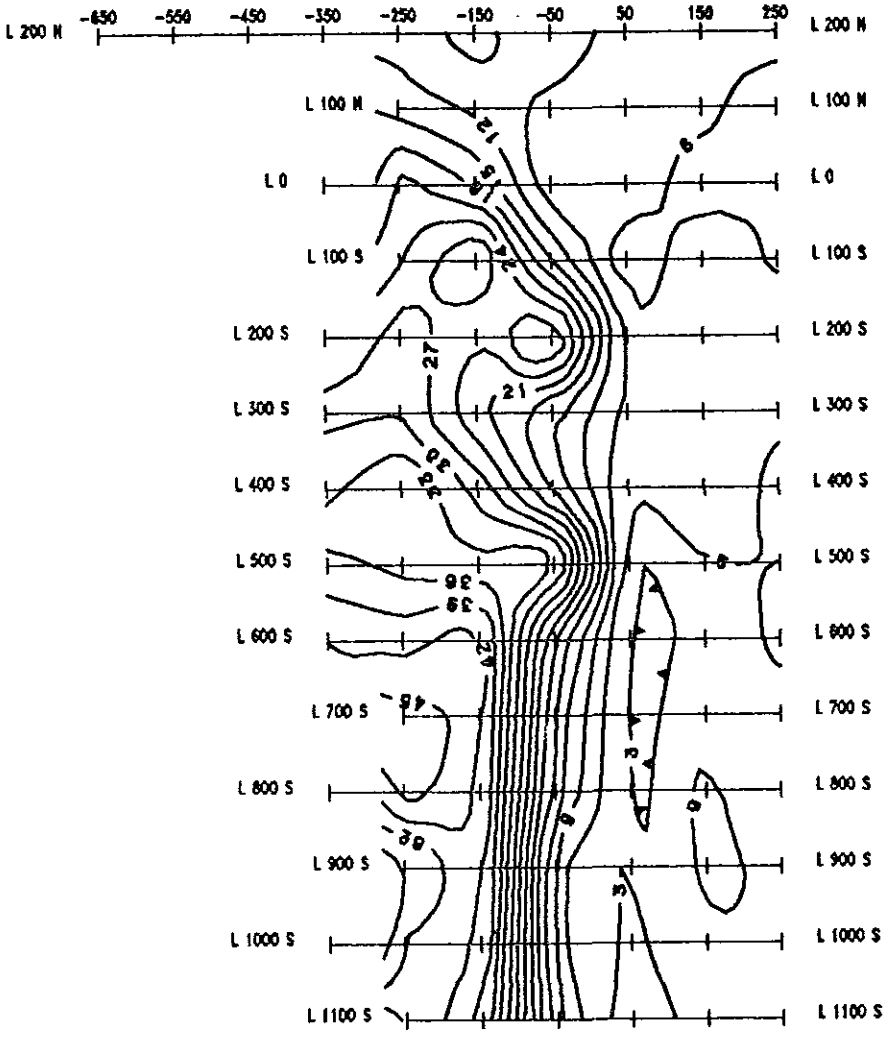

Fig. 7 Chargeability Plan Map, n=1

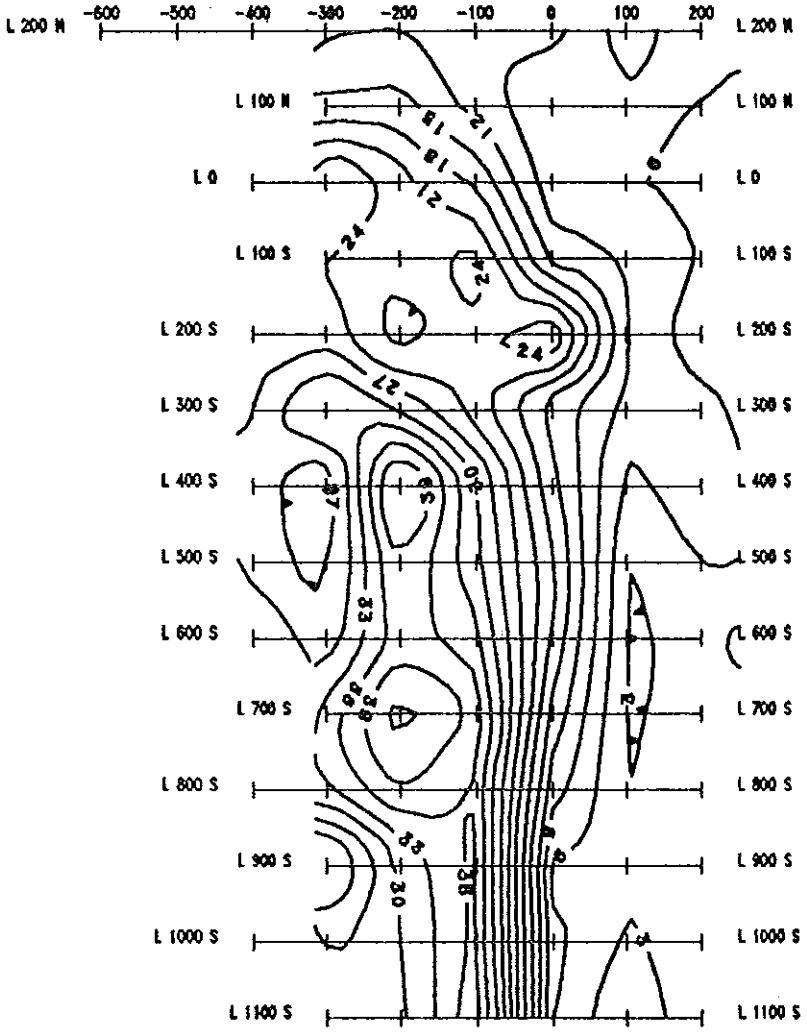

Fig. 7 Chargeability Plan Map, n=2

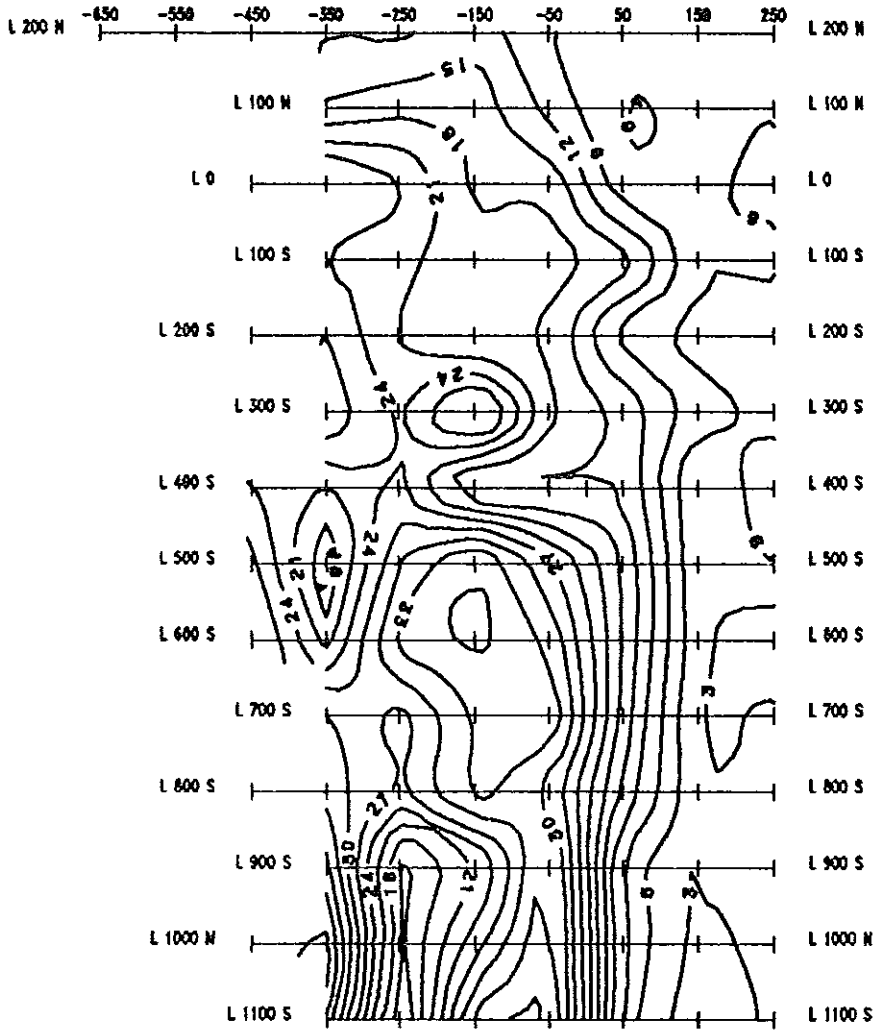

Fig. 7 Chargeability Plan Map, n=3

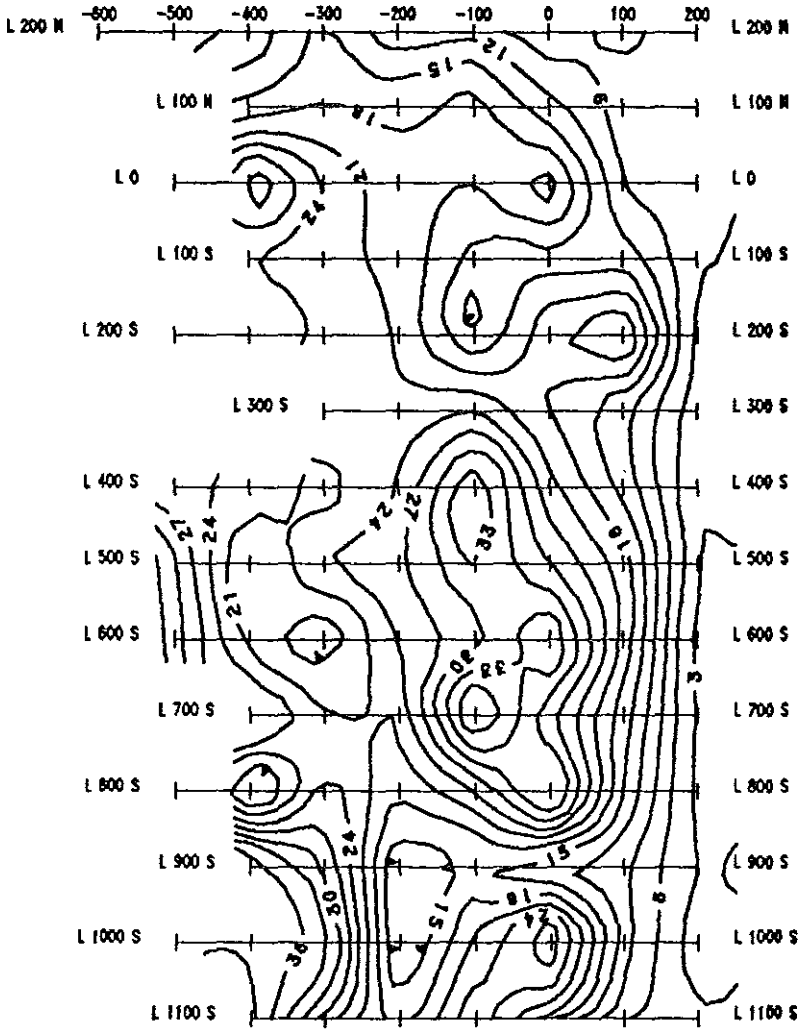

Fig. 7 Chargeability Plan Map, n=4

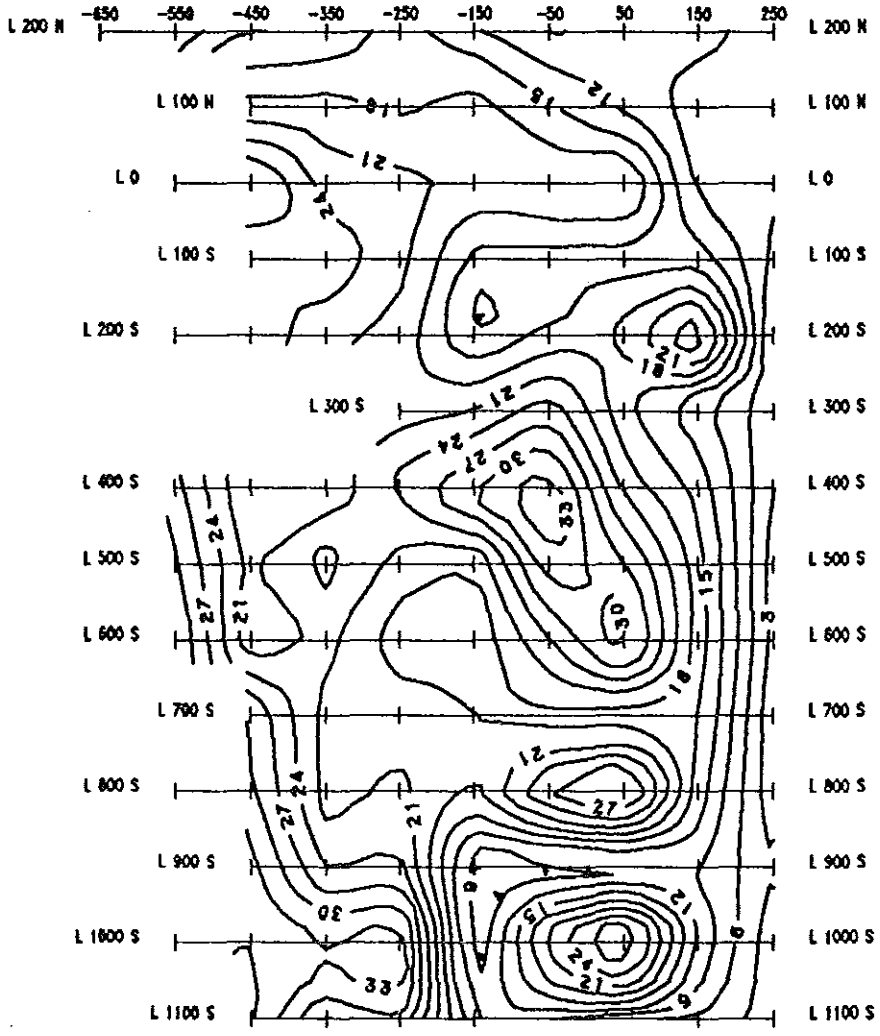

Fig. 7 Chargeability Plan Map, n=5

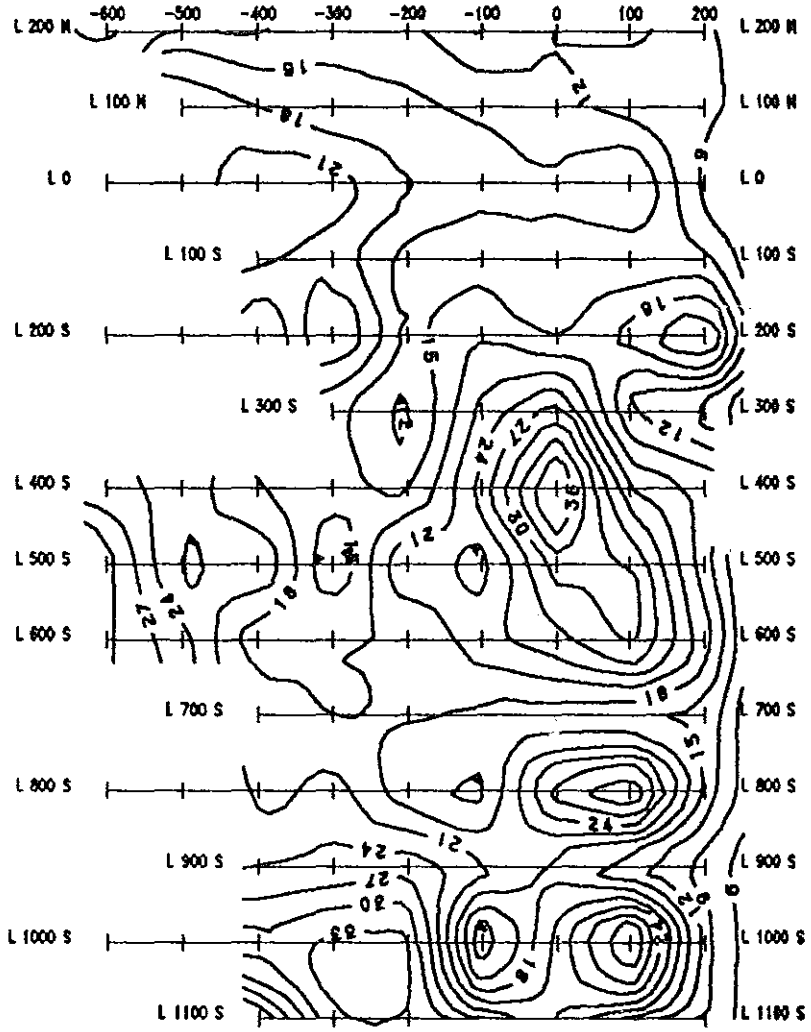

Fig. 7 Chargeability Plan Map, n=6

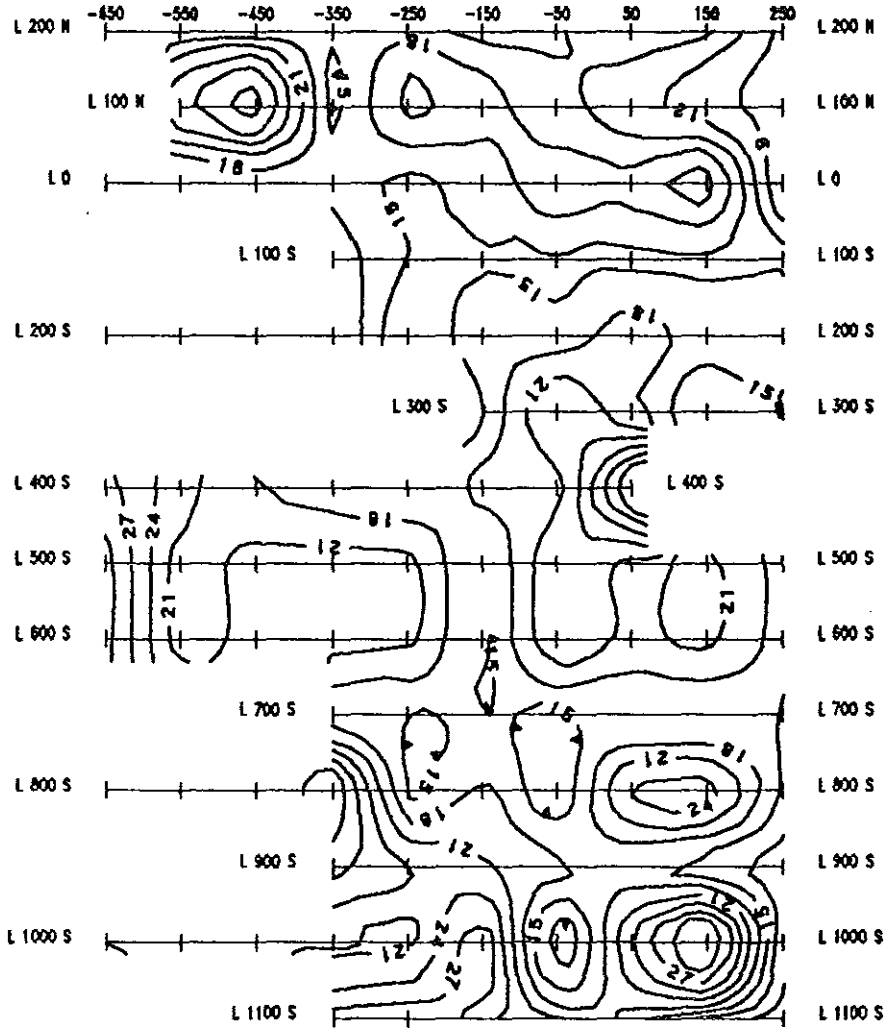

Fig. 7 Chargeability Plan Map, n=7

4: EM AND MAGNETIC SURVEYS

4:1 Introduction

In the re-evaluation phase, a number of anomalous zones and subsurface structures have been identified on the result of the IP/Resistivity survey. These zones were further tested and interpreted in detail. In this chapter the geophysical methods being employed for this extensive examination are discussed and new results are cited. These include identifying the fracture zones and determining the mineralized areas based on further diagnosis of the magnetic and EM methods.

The study of magnetic properties of rocks has several applications in applied geophysics. Measurements of local geomagnetic anomalies to outline subsurface structures and mark ore deposits are the principles applied as the basis of magnetic survey in this research work. In the first application, magnetic properties of rocks and the influence of tectonic zones on the quantity and distribution of magnetite in rocks play an important role to distinguish structural patterns. The second application, on the other hand, makes use of the spatial relationship that exists between stratiform base metal sulphides and magnetite formation. The absence of this association seems more of an exception than the rule, at least among volcanic associated massive sulphide deposits. Needless to say, the EM method best serves the purposes of the study, where metallic ores are being primarily sought. As is well known, base metal bearing ores fall into the anomalous bodies with high electrical conductivity that produce strong secondary electromagnetic fields.

4.2 general principle

Although most rock forming minerals are paramagnetic, certain rock types contain ferromagnetic minerals. The distribution of these magnetic minerals determine the distortion level of the geomagnetic field in an area. Interpretations of the geomagnetic field distortion in either of the stated investigation work, however, require sound knowledge of the basic principles relating magnetic minerals to geological structures and to ore environment. A full discussion of this important issue is given by Grant (1984/85). The article is a culling of materials from geological literature so organized that it can offer practical guidance to magnetic data interpretation in mineral exploration and to the study of geological structures. Summary of the basic ideas worthwhile to this particular study are outlined in the following.

All the common magnetic minerals, except for pyrrhotite, are within the Fe-Ti-O system. Some of the major magnetic minerals are magnetite, titanmagnetite, titanhematite, maghemite, pyrrhotite and native iron or Fe-Ni-Co alloys. Of these, magnetite is by far the most important in terms of abundance and large magnetic susceptibilities. Thus, magnetic survey, in practical terms, map magnetite distribution in rocks. The Other oxides of iron and titanium have, however, such small susceptibilities that their contribution to magnetic anomaly can be ignored. Furthermore, magnetic susceptibility of rocks are found to be directly proportional to their magnetite content. But that magnetite is not an inert mineral, its reactions with the environment highly affect the magnetic properties of a rock. Moreover, it is a minor constituent that forms rarely more than one percent by volume and its variation level seldom correlated with lithological division. For these reasons, magnetic measurement alone could not be a reliable lithological tracer, or it can

tell one very little about the mineralogy of rocks. Nonetheless, apart from lithological distinction, quite many ground truths can be inferred from magnetic data.

Therefore, to the useful end in magnetic interpretation, a good knowledge of the various factors that affect the magnetic properties of a rock has no option. Grand has cited local iron content, oxidation state, initial crystalization environment, degree of metamorphism and silica saturation to be in the hierarchy of influencing factors. In other words, these determine the magnetite content in a given lithologic unit. In this regard, vastly more complicated mineralogy of rock magnetism is given relatively little importance. Besides these intrinsic rock properties, there are certain exogenous conditions that tend to increase or decrease magnetization of rocks. Mechanical deformation, repeated metamorphism, and high temperature hydrous alterations all lead to an increase in magnetization of rocks either by increasing the magnetic susceptibly or by creating new magnetite, while low temperature alteration process, extreme oxidation and granitization or metasomatism tend to destroy magnetite.

The proportion of magnetite in igneous rocks tends to decrease with increasing acidity so that acid igneous rocks, although variable in their magnetic behavior are usually less magnetic than the basic igneous rocks (Keary et al, 1984). In practice most of the crystalline rocks of igneous origin such as granite, basalt and gabbro are sufficiently magnetic to influence the geomagnetic field even when they are buried beneath thick overburden sediments (Vacquier, 1963). On the other hand, sedimentary rocks may contain a great deal of iron as hydrous ferric oxide, hematite and siderite, but may be deficient in magnetite. Low temperature, high oxidizing environment and sedimentation

process are responsible for little magnetite content in sedimentary rocks. Therefore unmetamorphosed sediments are practically non-magnetic (Grant, 1984/85). Secondary magnetite in metamorphic rocks is produced at all levels of regional metamorphism. Mostly it develops under rather low-grade condition by the conversion of hematite or under high-grade condition due to the breakdown of hydrous (Fe, Mg) silicates such as biotite and hornblende. Total iron content and oxidation state are the most important attributes of secondary magnetite formation. The first fixes an upper unit on the potential productions, while the second controls the partitioning of iron between the oxide and silicate phases.

As mentioned earlier, local distortion in the geomagnetic field would be used to study subsurface structures and for prospecting purposes. Nothing has so far been said how these geological features are related to the quantity and distribution of magnetite in rocks into useful form. In this topic again, Grant (1984/85) in his second article offers an excellent discussion. Redeposited ores, the probable case of mineralization in Katta, in veins and fractures are associated with

a. major faulting with associated shear and fracture zones.

b. extensive zones of alteration usually but not always, associated with the above

c. post kinematic intrusions which act as heat sources to drive the ore bearing fluids through the conduits.

These structural setups are suitably prepared sites to receive many epigenetic types of ore deposits. Thus, one of the indirect tactical approach in ore prospecting happens to be a matter of tracing and mapping ground structures. These structures are also related to the magnetite content in two ways. First, tectonic zones in which major faulting and

fracturing have occurred are more permeable to weakly oxidizing or reducing aqueous solutions that, if they pass through in sufficient quantities, may cause chemical alteration along their path. On the other hand, ground water descending into shear or fracture zones will cause magnetite to oxidize into hematite, thus lowering the magnetic intensity along the fault zone. On the other hand, hot solutions rising through these weak zones towards the surface may lead to an increase or decrease the magnetite pattern. Generally, it would seem that the quantity of magnetite in tectonic zones may be enhanced or diminished depending upon the nature of aqueous solution. Second, the much more direct relation particularly in prospecting massive sulphide deposits, reduces to the association between magnetite and deposition environment of ore bodies discussed earlier topic.

Another magnetic feature of rocks is remanent mignetization-a nuisance in the interpretation of magnetic data. The inherited magnetization remaining after the removal of an applied field is known as remanent or permanent magnetization.[13] Primary remanent magnetization may be acquired either as an igneous rock solidifies and cools through the curie temperature of its magnetic minerals or as the magnetic particles of sediment align with in the earth's field during sedimentation. Secondary remanent magnetization may be impressed later in the history of a rock as magnetic minerals recrystallize or grow during diagenesis or metamorphism(Keary et al, 1984).

One of the main purposes of the EM method is to search for conducive ore bodies, whose conductivities are much greater than the host medium. Ores like graphite, pyrrhotite, pyrite, chalcopyrite, galena, magnetite, and arsenopyrite, are good conductors of electricity, and hence are suitable targets of EM methods (Parasnis, 1975). The

method, however, suffers from the drawback that such a high anomaly can be caused by disturbing bodies of largely minor interest located near the surface in the survey area. These anomalous fields could be caused by non-economic conductive sources or have different origin such as man made or magnetotelluric noise. Graphite and water filled shear zones, for example, are a nuisance non-economic conductive sources.

4.3 elementes of EM and magnetic methods

4.3.1 magnetic method

A scalar magnetometer measures the earth's total magnetic field, B_r. This field may be expressed in terms of its component as.

$$B_r = B_o + \Delta B$$

where B_o is the normal geomagnetic field at the measuring position, and ΔB is the anomalous magnetic vector setup as a result of induction, permanent magnetization, diurnal variation, secular effect, etc.

The geomagnetic field at any point on the earth's surface can be completely specified by the geomagnetic elements. These include the horizontal field, **H**; the vertical field, **Z**; and the declination, **D**. Among these magnetic elements, **D** is the least sensitive to changes in the dimensions and magnetic properties of subsurface body. It is therefore never used by itself in accurate magnetic work. Of the remaining, namely **H**, **Z** and **B** any one or more

can be chosen for measuring the respective anomalies ΔF, ΔZ, and ΔB. The anomaly vector in the total field is

$$\Delta B = B_r - B_o$$

and its magnitude is

$$|\Delta B| = |B_r - B_o|$$

$$= (\Delta Z^2 + \Delta H^2)^{1/2}$$

Since a proton magnetometer measures only magnitudes of the total field, B_r; and the main field, B_o; is practically estimated from International Geomagnetic reference field (IGRF) maps, and the anomaly actually calculated in geophysical prospecting is

$$\Delta B = |B_r| - |B_o|$$

$$= (H_r^2 + Z_r^2)^{1/2} - (H_o^2 + Z_o^2)^{1/2}$$

Let the anomaly produce a vertical component ΔZ and a horizontal component ΔH at an angle α to H_o. Only that part of ΔH in the direction of H_o, namely $\Delta H'$, will contribute to the anomaly (Keary et al, 1984).

$$\Delta H' = \Delta H_o \cos \alpha$$

Thus,

$$|Br|^2 = (|B_o| + |\Delta B|)^2$$

$$= (H_o + \Delta H')^2 + (Z_o + \Delta Z)^2$$

If this equation is expanded, the relationship between the geomagnetic elements, namely $B_o = H_o + Z_o$, are substituted and the insignificant terms in Δ ignored the above equation reduces to

$$\Delta B = \Delta Z \left(\frac{Zo}{Bo}\right) + \Delta H' \left(\frac{Ho}{Bo}\right)$$

Substituting the relations: $\Delta H' = H_o \cos \alpha$, $\sin I = Z_o/B_o$, and $\cos I = H_o/B_o$, yield

$$\Delta B = \Delta Z \sin I + \Delta H \cos I \cos \alpha$$

where I is the inclination of the geomagnetic field.

This approach can be used to calculate the magnetic anomaly caused by magnetic bodies represented by dipole, monopoles and 2-D configurations to be compared with total field anomalies observed by total field magnetometers.

4.3.2 EM method

Distortions in the intensity and direction of a primary field may be analyzed in terms of subsurface conducting features in a manner analogues to the study of geomagnetic distortions considered earlier. The amplitude-phase relationship between the primary and distorting (secondary) fields at the receiving position are best explained with the help of vector diagrams, which are found almost in all standard geophysics text books. Interested readers may refer to one of these books for the diagram and further discussion. Otherwise, a phase difference of $(\Pi/2 + \Phi)$ is introduced between the primary and secondary fields due to inductive coupling between the transmitter and the conductor in the subsurface, and electrical properties of the conductor (Telford, 1976). On the other hand, the mathematical problem of propagation, attenuation and generation of EM fields are governed by the Maxwell's equations. Assuming a harmonically varying quasistationary field [$\exp(-j\omega t)$] the Maxwell's equations in isotropic homogeneous media reduces to

$$\nabla \mathrm{X} \mathbf{E} = j\mu\omega\mathbf{H}$$

$$\nabla X H = \sigma E$$

$$\nabla \cdot H = 0$$

$$\nabla \cdot E = 0$$

The above relations again assume a form of the wave equations when taking Curl of the first two equations and making use of the vector identity Curl Curl F + grad div F-$\nabla^2 F$, i.e.

$$\nabla^2 E = |\sigma\mu\omega E$$

$$\nabla^2 H = |\sigma\mu\omega H$$

These equations govern the propagation of quasi-static electric and magnetic fields in an isotropic homogeneous medium.

If a plane-polarized magnetic field is considered to be traversing in the x-direction and varying sinusoidally with time; such simplification may give a good insight about the fundamental solution of the EM wave equation. The solution for such a case will be

$$Hy = Ho \exp[-az + |(\omega t - az)]$$

Where, $a = \sqrt{(\omega\mu\sigma/2)}$

The factor exp(-az) characterizes the attenuation of the wave with propagation distance, Z. This indicates that the magnetic field will propagate through a given medium without much attenuation when the quantity $\sqrt{(\omega\mu\sigma/2)}$ is small and vice versa (Ibid).

beginning and end of each profile survey, repetitive measurements were recorded at a base station established in the outskirts of the survey area.

In the EM survey, only five profiles from 100S to 500S were covered because the time for the field work allowed the survey to be carried out on these lines. The IGS-2/EM-4 working in the GENIE mode is employed, and two amplitude ratios for a pair of frequency signals have been recorded at each observation station. The GENIE mode comprises three components: the receiver, sensing coil and the transmitter. The reference and signal frequencies were generated by the TM-2 portable EM transmitter and the ratio change was measured using the IGS-2/EM-4 receiver; both instruments are of Scintrex produce. A reference frequency of 112.5 Hz and signal frequency of 337.5 Hz; and another reference frequency of 337.5 Hz and signal frequency of 3037.5 Hz were selected for the survey. The transmitter receiver separation was kept at 100 m spacing and reading was taken at 10 m picket interval. The traverse lines were in the east-west direction perpendicular to the baseline with 340^0 azimuth.

4.4.2 data processing

The magnetic field data were corrected for diurnal variation by adding or subtracting the amount dt/T from each measurement where d is an increase or decrease in readings at base station during an interval T, and t is the time at which measurement was taken after the initial base station reading. In order to compute the magnetic readings and EM data at regular points of gridding system, an automatic computer program working on the principle of bicubic spline interpolation method was used. Total field contour map is

finally prepared at a scale of 1:4000 and contour interval of 50γ have been chosen based on the data density.

Furthermore, profile plots have been generated for each frequency pair of the EM data, with the midpoint between the transmitter and receiving coil reckoned as the observation point.

4.4.3 Interpretation

4.4.3.1 magnetic interpretation

Fig. 8 represents a map of magnetic data obtained from profiles 100S to 600S. In places where Precambrian metamorphic and igneous rocks are prevalent, high frequency magnetic effects originating from near surface sources usually dominate the anomaly map. The magnetic map also contains highs and several low amplitude, and short wavelength anomalies that are evidently controlled by localized bodies of different nature. The map comprises two major conspicuous features: linear magnetic lows of different level and magnetic highs confined to the southern of the map. Both features are of prime interest in this research study for they are manifestation of the underground structure and mineralization in the study site. In addition, it can be noteworthy the weak anomalies lying just along profiles 100S.

Magnetic data are often used to locate the boundaries of rock units either having differing magnetic content or otherwise. These boundaries, in parables of structural geologists, are of faults, lithologic contacts, shear zones, fractures, fissures, etc. The first part of this

section deals with the results of magnetic survey in efficiently tracing the linear trend of such weak zones.

Nearly linear magnetic minima shown and mentioned earlier are attributed to a shear zone trending in the SE-NW direction. For comparison with this belt of low magnetic intensity, the zone is characterized by high resistivity gradient in the resistivity pseudosection and surface contour. The negative peak values, beyond a sharp drop to the background level, obtained in some locations along the zone entail more explanation than the possible association of magnetic minima not unusual to such structures. Hankel and Guzmen (1977) have thoroughly investigated this phenomenon and obtained petrophysical explanation to the situation. They made in situ magnetic susceptibility measurement and studied the content of opaque minerals in polished section. As a result, they found a sharp drop in magnetic susceptibility by a higher factor than the decrease in remanent magnetization which, in effect, resulted in the relatively high Q-value. This mild effect in the remanent magnetization is said to be due to several factors such as:

(1) Stability of the remanent component during oxidation.

(2) a created chemical remanence in the hematite.

(3) a created remanence in the smallest magnetite residuals.

However, the dominating effect on the sharp decrease of the susceptibility and hence increased Q-value, is due to the oxidation process that led to an increase of hematite at the expense of magnetite. In such situations, the content of Fe-hydroxide can also be considerable, indicating that the magnetite has also been hydrated. Therefore, the degree of martitization and hydration is the cause for the variation of susceptibility. Both

processes indicate near-surface alterations at low temperature, high oxygen and the presence of water. The lower magnetic minimas and the associated negative peaks may therefore be ascribed to oxidation, hydration and increased Q-value along the shear zone.

For the magnetic low belt, consolidating ground evidences are observed during the survey. Gossan of probably limonites and magnetite bearing crop out in a definite direction that trends approximately along the sharp magnetic gradient in the central-east part of the contour map. From general experience, structures of very low magnetic relief in magnetically disturbed environments have important implication in prospecting for mineral ores.

Anomaly maxima is clearly distinguishable between profiles 500S and 600S. This zone is associated with IP peak (Fig. 6) and involve pyrite-chalcopyrite mineralization as proved by the diamond drilling carried out earlier. The fact that the susceptibility of these ore minerals is too low to create such anomaly peaks would lead one to attribute this effect to the presence of magnetite in the indicated region.

Besides these main maximas, the magnetic map includes low and weak anomalies mainly along profile 100S. They are partly outlined in the IP contour maps, and their probable causes have been discussed in the IP interpretation part. Profile plots from EM data also show much more conspicuous anomalies between profile 100S and 200S. The interpretation is thus left to the forthcoming section that deals with the EM survey result.

4.4.3.2 EM interpretation

Field curves for the profiles from 100S to 500S are shown in Fig. 9. The ratio change at 337.5Hz and 3037.5 Hz signal frequencies with their respective reference frequencies of 112.5 and 337.5 are plotted for each traverse. The theoretical model response curves given in GENIE interpretation manual were derived from three model types including dipping thin plate in a non-conductive host. These have been generated using a plate program as developed by the Geophysical Laboratory of the University of Toronto (Scintrex Limited, 1986). For the qualitative interpretation of the field results, we use this catalogue of curves generated for the plate model.

The similarity between the theoretical curves for dipping plate and the field data of profiles 100S, 200S, and 300S, particularly for the 3037.5/337.5 frequency pair, is striking. It appears that conducting bodies are present west of the baseline at shallower depth. The possible graphitic zone outlined by the IP survey is supposed to give rise to the GENIE anomaly curves found in profiles 100S and 200S, whilst the anomaly in profile 300S has a different origin. The disparity of the positive peaks in the response curves over profiles 100S and 200S indicates that the graphite lens is dipping towards east. The anomaly on profile 300S is, however, correlated to copper mineralization as proven from geochemical sampling and bore hole 9, and 9B (Fig. 4) sank about 20 m west of the baseline along the profile (Ball, 1982). From the geological map, profile 300S is found to lie just over weathered fracture zone that has probably undergone supergene enrichment (Ibid).

The nature of the response curves for profiles 400S and 500S is quite different from the earlier case. No significantly similar model curves could be obtained for these field curves. Thus, the following interpretation scheme is mainly made based on the model response results stated in the discussion part of the GENIE interpretation manual: The positive shoulder flanked by peak minima on either side of the response curves observed in both profiles involve depth relationship of the conducting body to coil separation (L). It is described that when large value of L, as much larger as 1.5h (h-depth depth to target), is maintained the minima peaks tend to attain negative values, each centered approximately over one edge of the body. Since the response curve over profile 400S mets these conditions, the causative body is estimated to have about 185 m dimension in the east-west direction, and buried at about 70 m beneath the surface. As the log result at borehole No 4 (AZ 60, Inclination-45°, assumed coordinates 413 S, 104 W relative to the baseline) also indicates, a zone of scattered chalcopyrite with pyrite mineralization is intersected approximately between 138 m and 188 m in chlorite schists; which corroborates the estimated depth. Finally, regarding the choice of frequency pairs, It would be possible to say that the 337.5/ 211.5 Hz pair is found to be inappropriate, except in certain conditions where the conductor lies at very shallow depth. The other frequency pair, though It has enable the survey to map most of the conductive zones effectively, it has also missed some mineralized zone that may have economic importance owning to its limited depth of penetration. As shown earlier in the IP contour maps relatively deeper anomalous bodies along profile 200S (East of the base line), 400S, 500S and 600S have been identified which are not clearly shown in the EM profile plots.

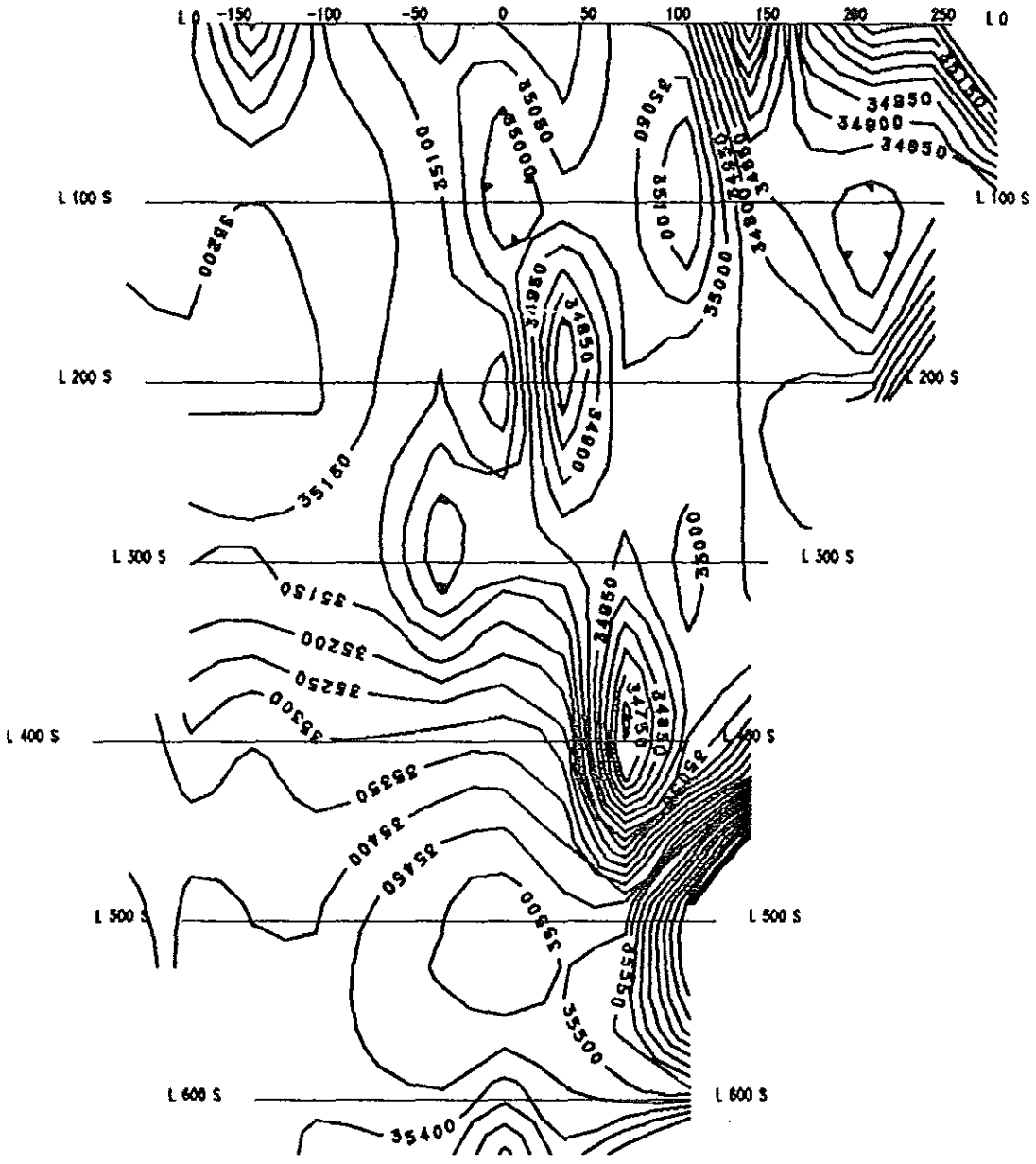

Fig.8 Magnetic Contour Map

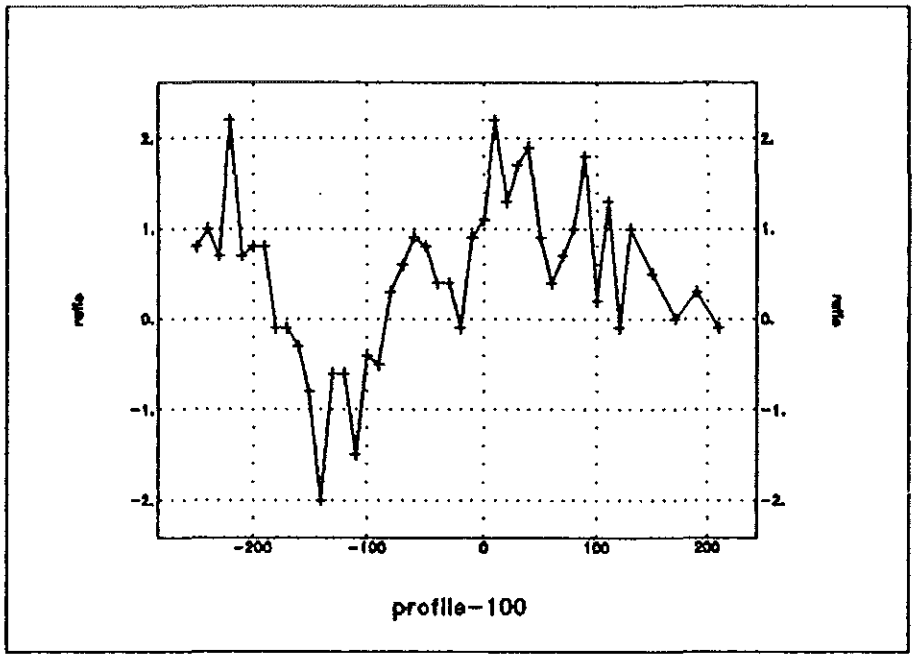

Line 100S for f_s=337.5 Hz and f_r=211.5 Hz

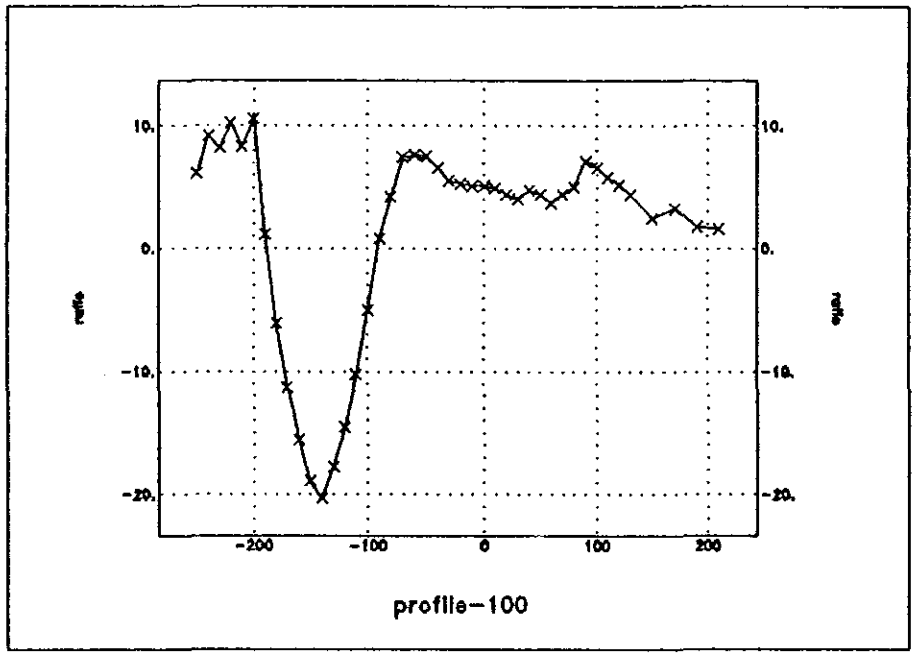

Line 100S for the f_s=3037.5 Hz and f_r=337.5 Hz

Fig. 9 EM profile plots

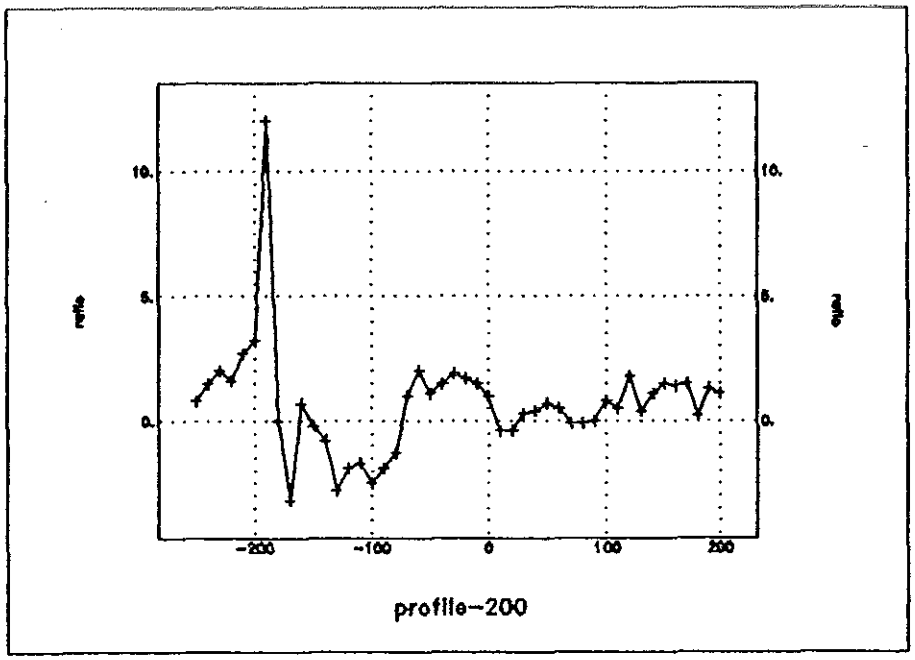

Line 200S for f_s=337.5 Hz and f_r=211.5 Hz

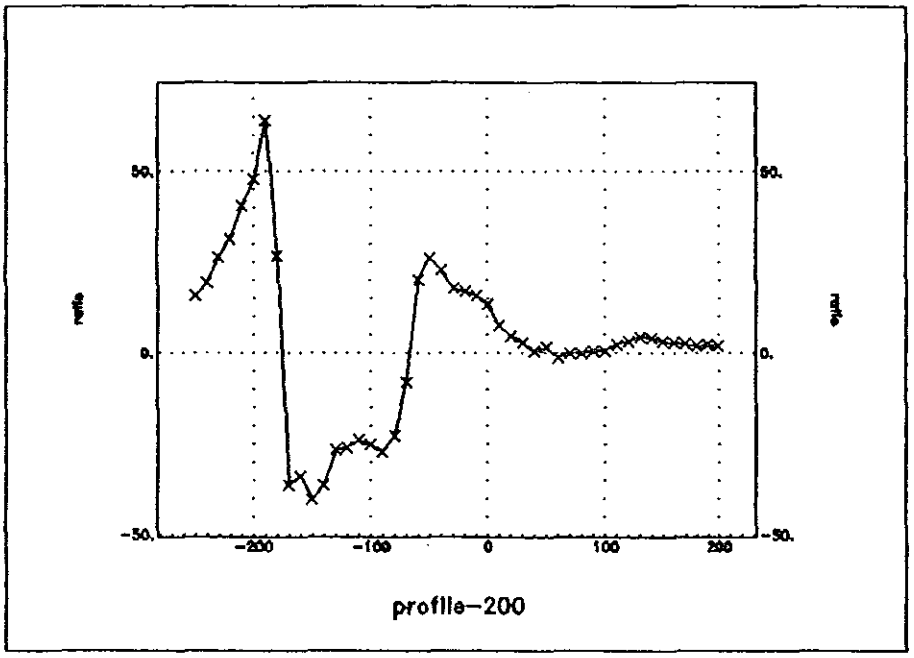

Line 200S for the f_s=3037.5 Hz and f_r=337.5 Hz

Fig. 9 EM profile plots

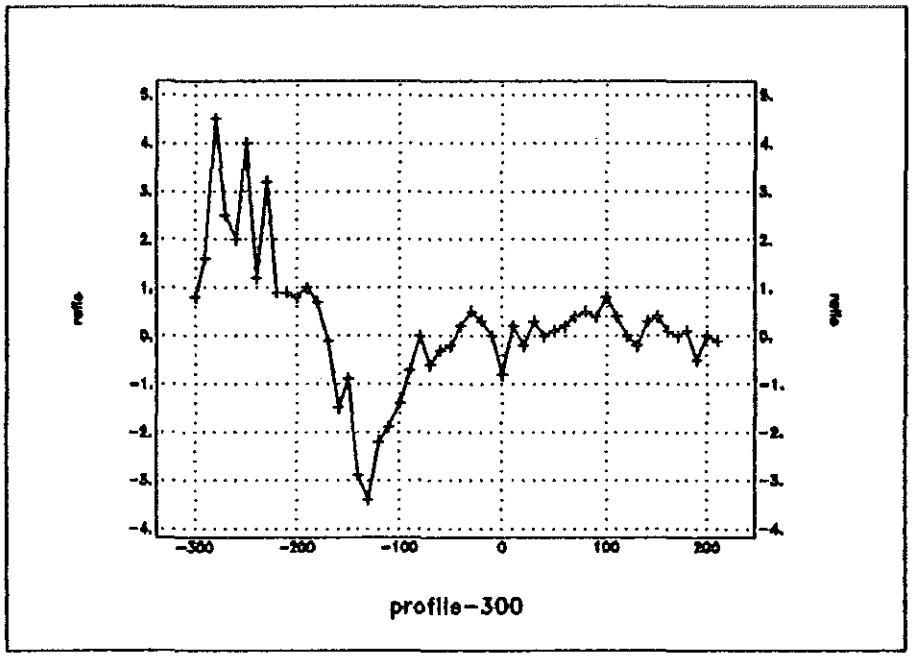

Line 300S for f_s=337.5 Hz and f_r=211.5 Hz

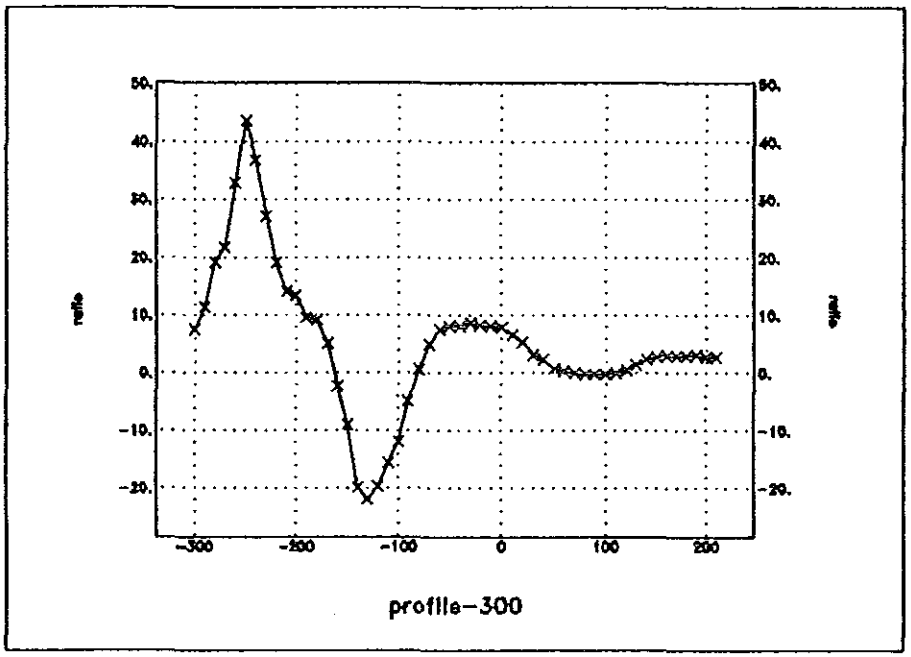

Line 300S for the f_s=3037.5 Hz and f_r=337.5 Hz

Fig. 9 EM profile plots

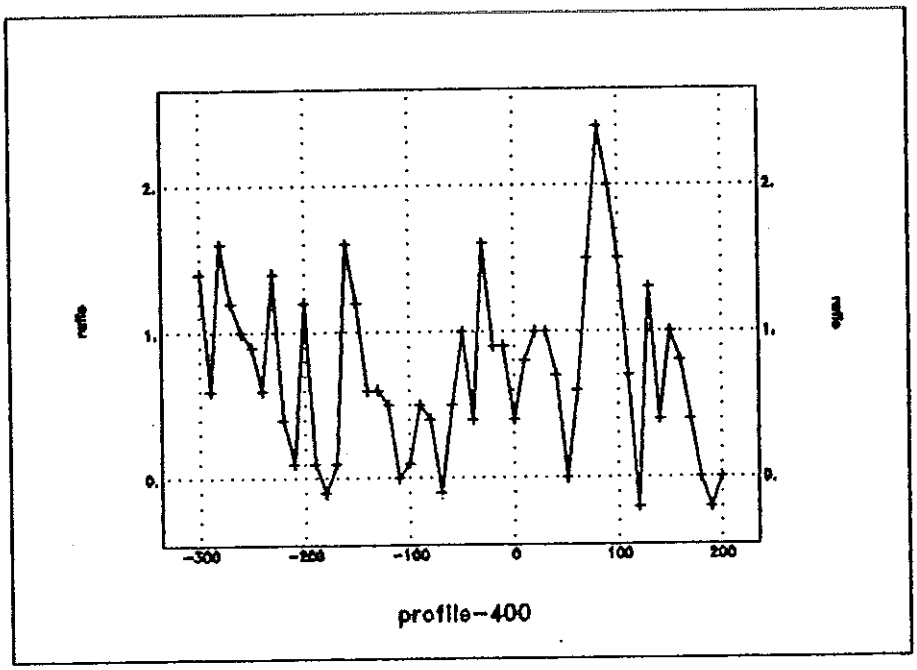

Line 400S for f_s=337.5 Hz and f_r=211.5 Hz

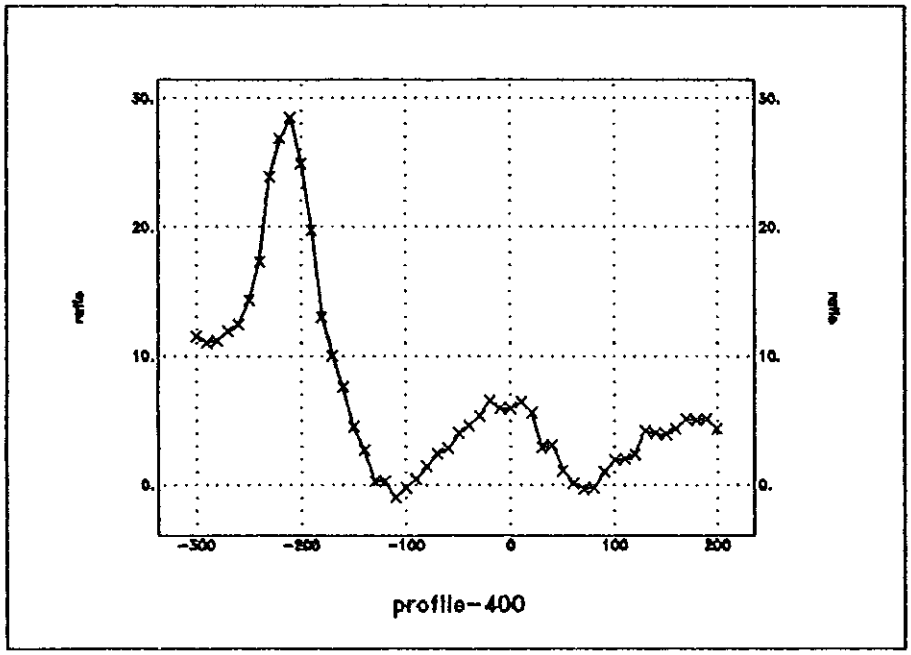

Line 400S for the f_s=3037.5 Hz and f_r=337.5 Hz

Fig. 9 EM profile plots

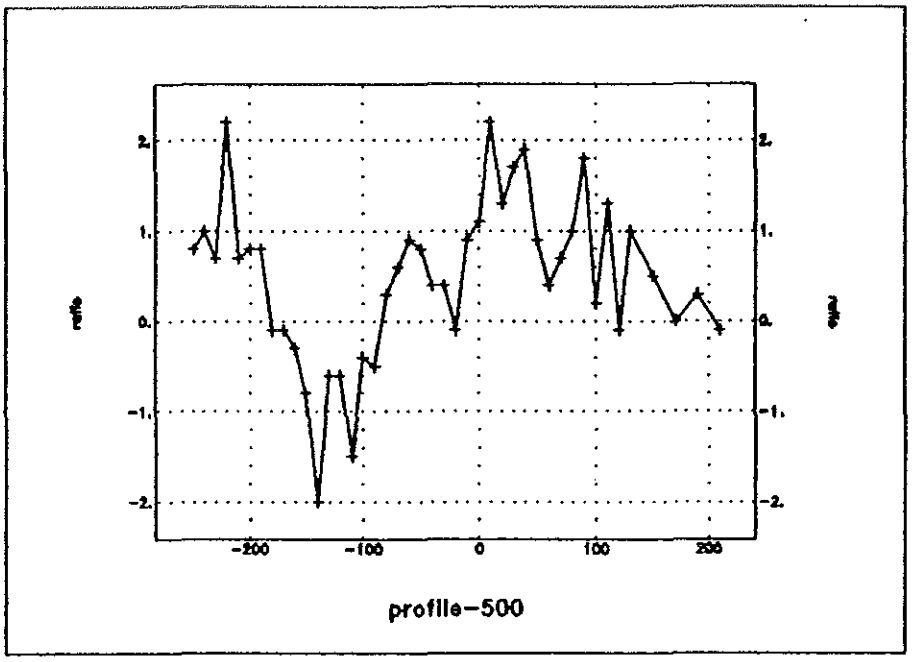

Line 500 for f_s=337.5 Hz and f_r=211.5 Hz

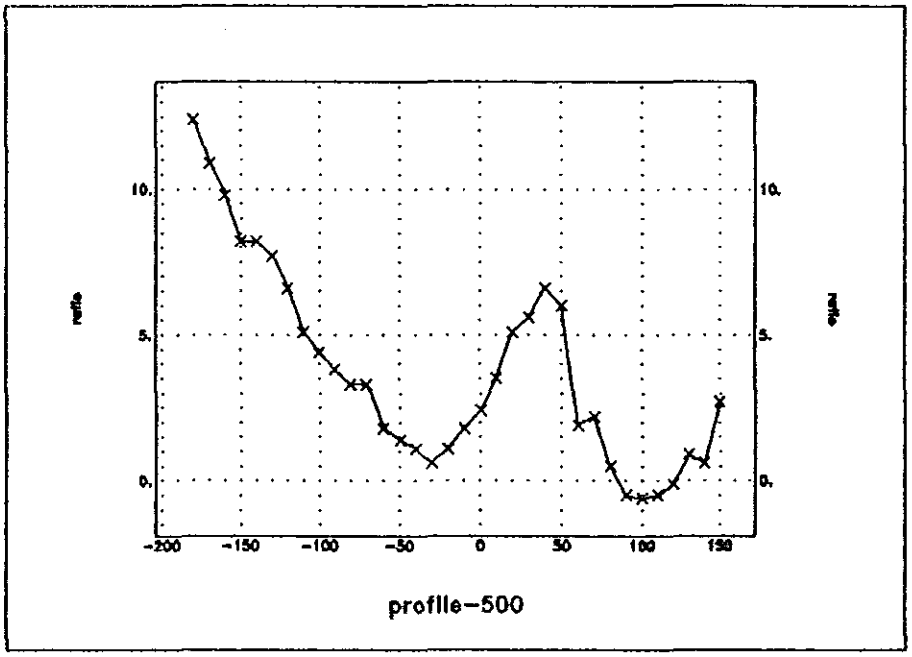

Line 500 for the f_s=3037.5 Hz and f_r=337.5 Hz

Fig. 9 EM profile plots

5. CONCLUSION AND RECOMMENDATION

5.1 conclusion

The most important and testing part in geophysical prospecting is the incorporation of separate geophysical results into one set of data system so that making good use of the integrated data will guarantee a reliable information about the targets sought. The structures and mineralized zones in Katta II are proof for the above assertion. The study has had two-fold objectives of delimiting the weak zones and investigating their association to base metal mineralization. Successful outcomes have been achieved in both cases.

Of the various correlations the most striking one is between the IP/resistivity pseudosection and the magnetic maps. The structural dislocation trending nearly in NW-SE direction reveals low magnetic zone that correlates well with high gradient contour in the IP/Resistivity pseudosection, thereby indicating the shear zone location. The shear zone has previously been indicated in many of the Geological maps of Katta area as inferred structure.

Another weak zone, which orthogoally intersect the previous shear zone, is also identified along profile 100S from the resistivity and magnetic maps. It is correlated very well with the shear zones in Fig. 3 that have a strike azimuth of 60^0-70^0 NE direction (Soukhoroukov, 1982).

The resistivity and magnetic methods are found to be best suited for ascertaining the shear zones, so are the IP and EM methods in the search for the ore deposits. Nevertheless, corroboration between the four methods was evident in certain instances. For example, anomaly responses from all the methods have consistently been observed between profiles 400S and 600S, the area that might have undergone supergene enrichment to yield the high grade chalcopyrite-pyrite ore body. Besides the underlain causative body along profiles 100S and 200S, that has been left doubtful as to whether it is graphite lens or not, has been outlined by the EM, IP and resistivity maps. In most cases, all methods show anomaly response over suspected zones of mineralization.

The work involves from identifying shallower depth anomalies through recognition of deep targets south of the survey area that may have economic importance, and their relation to the shear structures in the area. Thus, by comparing the results of the geophysical study made in Katta II with the available geological information, It is possible to make the following concluding remarks:

1. The geophysical anomalies observed along profiles 400S, 500S, 600S and probably also in the successive profiles could be associated with ore mineralization
2. The ore distribution appear to be structure controlled as they tend to be confined to fractures affected by weathering.
3. The most significant outcome of this study is that the fracture patterns are successfully identified and they are compatible to the existing geological results.

5.2 recommendation

In this paper, we have attempted to show the general nature of shear structures and their spatial relation to base metal mineralization based on integrated geophysical, geological and bore hole information. Perhaps the single most difficulty in this work was the abundance of graphitic schist in the area and the limitation in the application of electrical methods to discriminate it from the response of base metal bearing ore bodies. Additional work for understanding of the anomalous zones and quantitative description require an examination of a wide rage of geometrical and physical parameters. There are also important geometric properties of the Katta shear zone such as depth, width and strike extent that may need further consideration. This is obviously an area for further investigation both from academic and economic point of interest. In brief some of the tactical approaches we suggest that could be worthwhile in dealing with the above problems are:

1. Spectral study using the frequency domain IP and radiometric investigation of the suspected mineralized zones.
2. From qualitative assessment of the geophysical results, the low resistivity and high chargeability broad zone has been interpreted as depression zone. But, it may be verified if gravity survey is carried out and geological section is produced. Thus, this will be an interesting problem that may require further investigation too.
3. As far as the geometrical quantities of the shear zones are concerned they may be estimated if the available magnetic data is further processed and quantitatively interpreted.

REFERENCES

1. R.G. Park, Geological Structures and Moving Plates, (1995).
2. V. E. Camp 'Island Arcs and their role in the Evolution of the Western Arabian Shield' Geological Society of American Bulletin, 95, no.8, (1984).
3. V. Kazmin, 'The Precambrian of Southern and Western Ethiopia and some aspects of the Geology of the Mozambique Belt' (unpublished report, Library, Ethiopian Geological Survey, [1982]).
4. Y. T. Soukhoroukov, 'Geology and Geochemical Prospection for Copper, Zinc and Gold in Abo-Kami-Kata area, Central Wollega' (unpublished report, Library, Ethiopian geological Survey, [1971]).
5. Wahi, Ashok K., 'Geophysical Exploration for Base Metals in Kata, Tulu Chuche and Kutala areas, Wollega' (unpublished report, Library, Ethiopian Geological Survey, [1982]).
6. Tilahun Mammo, 'The Geology, Geochemistry and Origin of Sulphide Mineralization in Katta, Wollega province' (unpublished M.Sc. thesis, Addis ababa University, 1980).
7. de Wit M. et al, 'A Synopsis of the Geology around Katta, Wollega with recommendation for a drilling program' (unpublished report, Library, Ethiopian Geological survey, [1977]).
8. Holland, H. D., 'Granites Solutions, and Base Metal Deposits' Econ. Geology, 69, no.3 (1972), 281-301.
9. William L. Barrett et al, Introduction to Mineral Exploration, Anthony M. Evans (London: Blackwell science Ltd, 1995).
10. J.Wong, 'An Electrochemical Model of the Induced-Polarization in Disseminated Sulphide Ore' Geophysics, 44, no.7, 1979, 1245-1265
11. Joseph R. Hearst et al, 'Well Logging for Physical Properties' (McGraw-Hill,Inc.,1985)
12. W .J. Scott and G. F. West, 'Induced Palarization of Synthetic, High-Resistivity Rocks Containing Disseminated Sulfides' Geophysics, 34, no.1, 1969, 87-100.
13. P. Keary and M. Brooks, 'An Introduction to Geophysical Exploration'(Blackwell Scientific Publication, 1984).

14. M. Kuzvart, M Bohmer, 'Prospecting and Exploration of Mineral Deposits' Mirko Vanecek (Amsterdam: Elsevier Scientific Publishing Company, 1978).
15. George V. Keller, Frank C. Frischtnecht, ' Electrical Methods in Geophysical Prospecting' A. L. Cullen et at (Pergamon Press Inc., 1979).
16. Y. M. Kuznetsov, 'unpublished report, Library, Ethiopian Geological Survey)
17. D. C. Fraser, 'Contour Map Presentation of Dipole-Dipole Induced Polarization Data' Geophysical Prospecting, 29, no.4, (1981), 639-651.
18. R. F. Ball, 'A Brief Assessment of Drill Holes 3,4,5,6, 9 and 9B' (unpublished report, Library, Ethiopian Geological survey, [1982]).
19. F. S. Grant, 'Aeromagnetics, Geology and Ore Environments, I. Magnetite in Igneous, Sedimentary and Metamorphic Rocks, An Overview' Geoexploration, 23, no.3 (1984/85), 303-333.
20. V. Vacquier et al, 'Interpretation of Aeromagnetic Maps' (New York; Geological Society of America).
21. F. S. Grant, 'Aeromagnetics, Geology and Ore Environments, II. Magnetite and Ore Environments' Geoexploration, 23, no. 3 (1984/85), 335-362.
22. D. S. Parasnis, ' Mining Geophysics', second edition (Amsterdam; Elsevier Scientific Publishing Company, 1975).
23. D.S.Parasnis, 'Principles of Applied Geophysics', third edition (London:Chapman and Hall Ltd., 1979).
24. W. M Telford, et al, 'Applied Geophysics' (London; Cambridge University press, 1976).
25. Scintrex Limited, 'IGS-2/EM-4 and SE-88 Moving source GENIE Interpretation Manual' (Ontario: Scintrex Limited, 1986).
26. IGS-2/ MP-3/4 Proton Magnetometer System Operation Manual.
27. Henkel., H. and Guzman, M., 1977, 'Magnetic Features of Fracture Zones' Geoexploration, 15, no.3 (1977), 173-181.
28. Belay Desta, 'Katta Drill Hole DDK 7/8' (unpublished report, Library, Ethiopian Geological Survey, (1978))

DECLARATION

I, the undersigned, declare that my thesis being entitled is my original work and has not presented for a degree in any other University. Sources of relevant materials taken from books and articles have been duly acknowledged.

Name: AHEMAYEHU BERHE
Signature:

This thesis has been submitted for examination with my approval as University advisor.

Name: TIGISTU HAILE
Signature:
Date: 22 June 1998